

# Inertial frictional ratchets and their load bearing efficiencies

D. Kharkongor<sup>1,2</sup>, W.L. Reenbohn<sup>3</sup> and Mangal C. Mahato<sup>1,\*</sup>

<sup>1</sup>*Department of Physics, North-Eastern Hill University, Shillong-793022, India*

<sup>2</sup>*Department of Physics, St. Anthony's College, Shillong-793001, India and*

<sup>3</sup>*Department of Physics, National Institute of Technology Meghalaya, Shillong-793003, India*

(Dated: July 20, 2018)

## Abstract

We investigate the performance of an inertial frictional ratchet in a sinusoidal potential driven by a sinusoidal external field. The dependence of the performance on the parameters of the sinusoidally varying friction, such as the mean friction coefficient and its phase difference with the potential, is studied in detail. Interestingly, under certain circumstances, the thermodynamic efficiency of the ratchet against an applied load shows a non-monotonic behaviour as a function of the mean friction coefficient. Also, in the large friction ranges, the efficiency is shown to increase with increasing applied load even though the corresponding ratchet current decreases as the applied load increases. These counterintuitive numerical results are explained in the text.

PACS numbers: 05.10.Gg, 05.40.-a, 05.40.Jc, 05.60.Cd

---

\*Electronic address: mangal@nehu.ac.in

## I. INTRODUCTION

The present spurt in the research activity on thermal ratchets began with the experimental observation of asymmetric motion of protein molecules at a constant temperature along microtubules[1]. The idea of ratchets did, however, exist since long. The most popular among them being the thought experiment on ratchet and pawl by Feynman[2]. Of course, in this case the ratchet and pawl are kept at two different temperatures. Immediately after the biological experiment two important physical models were put forth: one by Prost and coworkers and named as flashing ratchet[3] and the other by Magnasco called the rocked ratchet[4]. Both these pioneering models use asymmetric periodic potentials and the particles are made to move in presence of thermal noise (nonzero temperature). In the case of flashing ratchets the potential is switched *on* and *off* for certain durations repeatedly so that during the off condition the particles diffuse symmetrically about the initial position of minimum of the initial well of the potential and during the on situation the particles roll down to the minimum of the present well of the potential. By suitably adjusting the durations of the off and on conditions depending on the temperature one achieves net (ratchet) current because the maxima of the potential on the left and right sides of a minimum happen to be located at different distances. On the other hand, in the case of rocked ratchet the system is subjected to a sinusoidal external forcing (null mean impulse per period). Since the potential is asymmetric the particles encounter different potential barriers when the forcings have different directions during a cycle leading to a net current. Both these models had overdamped initiations. A comprehensive review on ratchets is given by Reimann[5]. The scope of ratchet models has since been extended much further[6, 7].

The rocked ratchet model, with asymmetric periodic potential, was extended to underdamped systems for the first time by Jung and coworkers[8]. This pioneering work extended the possibility of ratchet effect in underdamped deterministic systems. Subsequently, the underdamped deterministic ratchet model has been investigated further[9–12]. There has since then been many extensions to this underdamped model and applied to many noise induced systems including Josephson junctions[13–15], the diffusion of adatoms on the crystal surface [16], dislocation of defects in metals[17] and to other important situations wherein instead of inactive particles self-propelling particles were considered[18, 19]. Later on the ratchet current was shown to be possible in symmetric periodic potentials as well using pe-

riodic but asymmetric drives again with null mean imposed impulse per period[21–23]. The asymmetric drive could be obtained in various ways. For example, a 'square-wave' drive with a large constant force for a small duration and a small constant force in the opposite direction for a longer duration[24] gives an appropriate asymmetric drive. A biharmonic drive being an another example[25, 26] of asymmetric drive used to obtain ratchet current in overdamped as well as underdamped symmetric periodic potential systems. In most of the cases, in order to obtain ratchet current the medium (substrate) is considered spatially uniform so that the friction coefficient is constant in space. With uniform medium, as discussed earlier, ratchet current is obtained either in an asymmetric periodic potential and rocked periodically in time or in a symmetric periodic potential but rocked periodically with a time asymmetric force of zero mean over a period. However, there is another important case where the medium is considered to offer nonuniform diffusion coefficient for the motion of the particle to obtain net asymmetric current.

In an important work, Büttiker[27] had shown that the effect of a periodically varying diffusion coefficient on a periodic potential of same period but with a phase difference is equivalent to making the periodic potential tilt with a constant mean slope. However, diffusion coefficient results from a combination of two quantities: temperature and friction coefficient of the medium. Thus either the temperature or the friction coefficient (or both) can be varied to obtain the desired diffusion coefficient. Nonuniformity of temperature automatically puts the system in nonequilibrium situation and as argued by Landauer[28] there will be asymmetric particle crossings over potential barriers even without the application of external drive. This result was also exploited to obtain ratchet current[29, 30]. Luchsinger[31], considered a similar system as Büttiker's model but instead of a space-dependent temperature field, the space-dependent diffusion was induced by a position-dependent mobility. In this overdamped case, a net current was attained by considering a two-state model with different transition rates in order that detailed balance may be broken. Friction coefficient, however, is ineffective in static equilibrium situations and it comes into play only when the particles are in motion. It is a weak agent and, unlike non-uniform temperature, needs simultaneous application of external drive to obtain ratchet current. Nevertheless, the nonuniform friction breaks the left-right symmetry if varied periodically as the potential but with a phase difference. In the present work we consider the friction coefficient to be periodic in space as the potential but with a phase difference.

A particle moving in a medium and experiencing space dependent friction depending on the inhomogeneity of the medium is not so unusual in nature. Wahnström, using a realistic Lennard-Jones interaction potential as a practical illustration, showed that the space dependence of friction appears because of coupling of adatom-motion degrees of freedom with the ionic vibrations on the surface of substrates[32]. Nonuniform friction can occur also due to nonuniform density of the medium through which the particle moves. For example, a periodic nonuniform density in air can be established by setting up a stationary sound wave just as in a Kundt's tube experiment. In addition if electric charges are placed periodically in a line such that the position of the charges do not coincide exactly with the projected nodes or antinodes of the stationary wave, then a charged particle moving along the line of nodes will experience not only a periodic potential but also a periodic variation of friction with somewhat shifted in phase. We thus have a model system that can be realized experimentally.

Ratchet effect has been obtained in symmetrically periodic overdamped[33–36] as well as underdamped[11, 24, 26, 37–39] frictionally nonuniform systems. In Ref.[36] the authors consider the motion of a dimer consisting of two components connected by a harmonic spring in the same periodic potential and external force environment but experiencing different friction coefficient. In Ref.[11, 24, 37, 39] the external periodic drive frequency were taken of the order of the mean rate of passages of the particle across the potential barriers. In the present work, for reason to be made clear later, we use larger frequency of period drive as in Ref.[26, 38]. We consider the motion of underdamped particles in a sinusoidal potential  $V(x) = -\sin x$  and driven by a sinusoidal external field  $F(t) = F_0 \cos \omega t$  with  $F_0 \ll F_c$ , where  $F_c$  is the critical field amplitude at which the barrier of the combined effective potential  $U(x) = V(x) - xF(t)$  just disappears. Since  $F_0 \ll F_c$ , the particles always encounter a finite potential barrier. It is the presence of thermal fluctuations that help the particles to overcome the potential barriers and nonzero phase difference  $\theta$  in the periodic friction coefficient  $\gamma(x) = \gamma_0(1 - \lambda \sin(x + \theta))$  leads to asymmetry in the barrier crossings to the left and right directions giving ratchet current. Here  $\lambda$  is the inhomogeneity parameter with  $0 \leq \lambda \leq 1$  and  $\gamma_0$  is the mean value of the friction coefficient  $\gamma_0$  over one period.

Since the frictional inhomogeneity is the only symmetry breaking agent considered, with  $\theta \neq n\pi$ ,  $n = 0, \pm 1, \pm 2, \dots$ , the underdamped ratchet yields only small currents and consequently has very small thermodynamic efficiency (defined as the ratio of work done by the system against an applied load to the total energy spent on the system). Admittedly,

the efficiency of the frictional ratchet considered in the present case is negligible compared to the maximal efficiency (mostly, Stokes efficiency) ( $>0.6$ ) obtained by Spiechowicz and coworkers[14, 15]. Interestingly, Ref.[14] shows that a symmetric periodic potential system driven by a temporally symmetric periodic force exhibits more efficiency when an asymmetric Poissonian white noise of mean  $\langle \eta(t) \rangle = F$  is applied than when subjected to a constant tilt  $F$ . The present work, however, is not about obtaining large ratchet currents or more efficient current rectification but how the thermodynamic efficiency changes as an externally applied load is changed for various  $\gamma_0$  and  $\omega$  values. Interestingly, it shows, for instance, under certain circumstances, some counter-intuitive result that the efficiency increases as an externally applied load is increased. (The numerical results will be presented in detail in a section in the following.) It is to be noted that overdamped frictional ratchets yield relatively much larger currents[33]. However, the overdamped ratchets, operating in a different domain of parameter space, do not show the kind of interesting results that we obtain in the present underdamped case.

In the present work, we explore the role of friction coefficient  $\gamma$  on the ratchet current and the thermodynamic efficiency of the frictional ratchet, though small in magnitude, sometimes shows seemingly counterintuitive results. For the purpose of obtaining the thermodynamic efficiency of the frictional ratchet, in addition to the sinusoidal forcing, we apply an external constant force (load) opposing the ratchet current. Naturally, the ratchet can sustain only a small load before the ratchet current vanishes and gives way to the constant force induced current in the direction of the load. This critical value of load increases with increasing value of the mean friction coefficient  $\gamma_0$ . In a previous work, unlike the symmetric potential used in the present case, currents were calculated in a sinusoidally driven asymmetric periodic potential by applying an additional constant load[40]. In that work, for small asymmetry parameter  $\Delta \leq 0.2$  of the potential, the applied load direction is such as to help increase the current. The purpose of the present work, however, as mentioned earlier, is to let the ratchet perform work against the load (current reducing load) and thereby investigate the thermodynamic efficiency of the ratchet.

In the next section II, the model of the system will be described. In section III we give a brief discussion on why spatially periodic variation of friction coefficient of the medium should yield ratchet current and also summarize some results of an earlier work which has direct bearing on the present work. The numerical results based on our present investigations

of the behavior of ratchet current and mean absorbed energy without and with load applied to the system will be presented in detail in Sec. IV. In the last section V our main results will be discussed and summarised.

## II. THE MODEL

We consider the motion of an ensemble of under-damped non-interacting Brownian particles each of mass  $m$  in a periodic potential  $V(x) = -V_0 \sin(kx)$  with  $V_0$  as the amplitude of the potential and  $k$  is its wave number. The medium in which the particle moves is taken to be inhomogeneous in the sense that it offers a spatially varying friction with coefficient

$$\gamma(x) = \gamma_0(1 - \lambda \sin(kx + \theta)) \quad (2.1)$$

that leads the potential by a phase difference  $\theta$ . Here,  $\lambda$  is the inhomogeneity parameter, with  $0 \leq \lambda \leq 1$  and hence  $\gamma_0(1 - \lambda) \leq \gamma(x) \leq \gamma_0(1 + \lambda)$ .

In addition, the potential is rocked by a sub-threshold periodic time-dependent forcing  $F(t) = F_0 \cos(\omega t)$ , with  $\omega = 2\pi/\tau$  as the rocking frequency and  $\tau$  as the rocking period and  $F_0$  as the forcing amplitude. The equation of motion of the particle subjected to a thermal Gaussian white noise  $\xi(t)$  at temperature  $T$  is given by the Langevin equation[41, 42],

$$m \frac{d^2 x}{dt^2} = -\gamma(x) \frac{dx}{dt} - \frac{\partial V(x)}{\partial x} + F(t) + \sqrt{\gamma(x)T} \xi(t). \quad (2.2)$$

with

$$\langle \xi(t) \rangle = 0, \langle \xi(t) \xi(t') \rangle = 2\delta(t - t'). \quad (2.3)$$

Here, and throughout the text,  $\langle \dots \rangle$  correspond to ensemble averages.

For simplicity and convenience the equation is transformed into dimensionless units[43] by setting  $m = 1$ ,  $V_0 = 1$ ,  $k = 1$ , with reduced variables denoted again by the same symbols. The Langevin equation therefore takes the form

$$\frac{d^2 x}{dt^2} = -\gamma(x) \frac{dx}{dt} - \frac{\partial V(x)}{\partial x} + F(t) + \sqrt{\gamma(x)T} \xi(t), \quad (2.4)$$

where the potential is reduced to  $V(x) = -\sin(x)$  and

$$\gamma(x) = \gamma_0(1 - \lambda \sin(x + \theta)). \quad (2.5)$$

Equation (2.4) is numerically solved (i.e., integrated using Ito definition) to obtain the trajectories  $x(t)$  of the particle for various initial conditions using Heun's method[44–46]. For initial positions  $x(t = 0)$  the period  $-\frac{\pi}{2} < x \leq \frac{3\pi}{2}$  is divided uniformly into either  $n = 100$  or, in some cases, 200 values (and hence  $n$  initial positions) and the initial velocity  $v(t = 0)$  is set equal to zero throughout in the present work.

For each trajectory, corresponding to one initial position  $x(0)$ , the thermodynamic work done by the field  $F(t)$  on the system (or the input energy) is calculated using stochastic energetics formulation of Sekimoto as [47]:

$$W(0, N\tau) = \int_0^{N\tau} \frac{\partial U(x(t), t)}{\partial t} dt, \quad (2.6)$$

where  $N$  is a large integer denoting the number of periods taken to reach the final point of the trajectory. The effective potential  $U$  is given by

$$U(x(t), t) = V(x(t)) - x(t)F(t). \quad (2.7)$$

The mean input energy per period, for a given trajectory, is given as

$$\overline{W} = \frac{1}{N} W(0, N\tau). \quad (2.8)$$

Since  $V(x)$  is not explicitly dependent on time, all of the contribution to  $W(0, N\tau)$  comes from the second term in  $U$ , Eq. (2.7).

$$W(0, N\tau) = - \int_0^{N\tau} x(t) \frac{\partial F(t)}{\partial t} dt, \quad (2.9)$$

Note that this relation is true even if a constant load is applied, replacing  $V(x) = -\sin(x)$  by  $V(x) = -\sin(x) + xL$ . That is the input energy with load  $W(0, N\tau, L)$  is equal to the input energy without load  $W(0, N\tau, 0)$ :

$$W(0, N\tau, 0) = W(0, N\tau, L). \quad (2.10)$$

However, though  $W(0, N\tau)$  does not explicitly depend on  $V(x)$ , the latter implicitly affects  $W(0, N\tau)$  through  $x(t)$ . Because of the nonzero phase difference between  $F(t)$  and  $x(t)$  the integral  $W(0, N\tau)$  is finite. The nonzero phase difference results in hysteresis  $\overline{x(\overline{F})}$ , whose area is a measure of energy dissipation per period by the system. The overall mean input energy per period,  $\langle \overline{W} \rangle$ , is calculated as an (ensemble) average over all the  $n$  trajectories (corresponding to all the initial positions considered). Again, we find that

the mean hysteresis loop area  $\langle \bar{A} \rangle = \langle \bar{W} \rangle$ . Similarly, the mean velocity  $\bar{v}$ , over one trajectory, is calculated as

$$\bar{v} = \frac{1}{N\tau}(x(t = N\tau) - x(t = 0)), \quad (2.11)$$

and the overall mean (net) velocity or the ratchet current,  $\langle \bar{v} \rangle$ , is calculated as the ensemble average over all the  $n$  trajectories. Typically, the value of  $N$  is chosen to have relatively small error bars so that the qualitative features of the results are not obscured.

### III. NONUNIFORM FRICTION AND RATCHET EFFECT: A SUMMARY

#### A. Why a periodically varying friction leads to ratchet current?

In this subsection, we present a qualitative discussion on why a spatially varying friction coefficient of the medium whose periodicity is same as that of the underlying potential function may lead to net asymmetric current when driven by a temporally symmetric periodic force field.

Figure 1 shows three curves: (1) the sinusoidal potential  $V(x) = -\sin x$ , (2) the effective potential  $U(x) = V(x) - xF(t)$ , where the external drive  $F(t) = F_0 \cos \omega t$  when (a)  $F(t) = -F_0 = -0.5$  and (b)  $F(t) = F_0 = 0.5$ , and (3)  $\bar{\gamma}(x) = \gamma(x) - 1$ , where the friction coefficient  $\gamma(x) = \gamma_0(1 - 0.9 \sin(x + \theta))$ , with  $\theta = 0.5\pi$ . We plot  $\bar{\gamma}(x)$  instead of  $\gamma(x)$  (here with  $\gamma_0 = 1.0$ ) for convenience of comparison. Notice that  $U(x)$  with  $F(t) =$  (a)  $-0.5$  and (b)  $+0.5$ , provide exactly the same potential barrier but in reverse directions. Therefore, if  $\gamma(x)$  were uniform or nonuniform with  $\theta = 0$  or  $\pi$  there would be no net particle current because particle would be equally likely to move either to the right or to the left. However, if  $\theta \neq 0, \pi$  the left-right symmetry is broken, that is, the particle encounters different situations in the two directions.

We focus attention on a period of  $\bar{\gamma}(x)$  with end points  $x = x_1$  and  $x = x_2$  corresponding to the two consecutive minima of the effective potential  $U(x)$  with intervening maximum at  $x = x_3$ . AB denotes the segment of  $\bar{\gamma}(x)$  from  $x_1$  to  $x_3$  and BC from  $x_3$  to  $x_2$ . In Fig. 1a with  $F(t) = -F_0 = -0.5$  in the segment BC the mean value of  $\bar{\gamma}(x)$  (or that of  $\gamma(x)$ ) is smaller than in the segment AB. Also, since in this case mean slope of  $U(x)$  is positive it is more likely for the particle to move to the left (from  $x_3$  towards  $x_1$ ). In Fig. 1b the situation is exactly the reverse. However, from Fig. 1a it is clear that in the former case

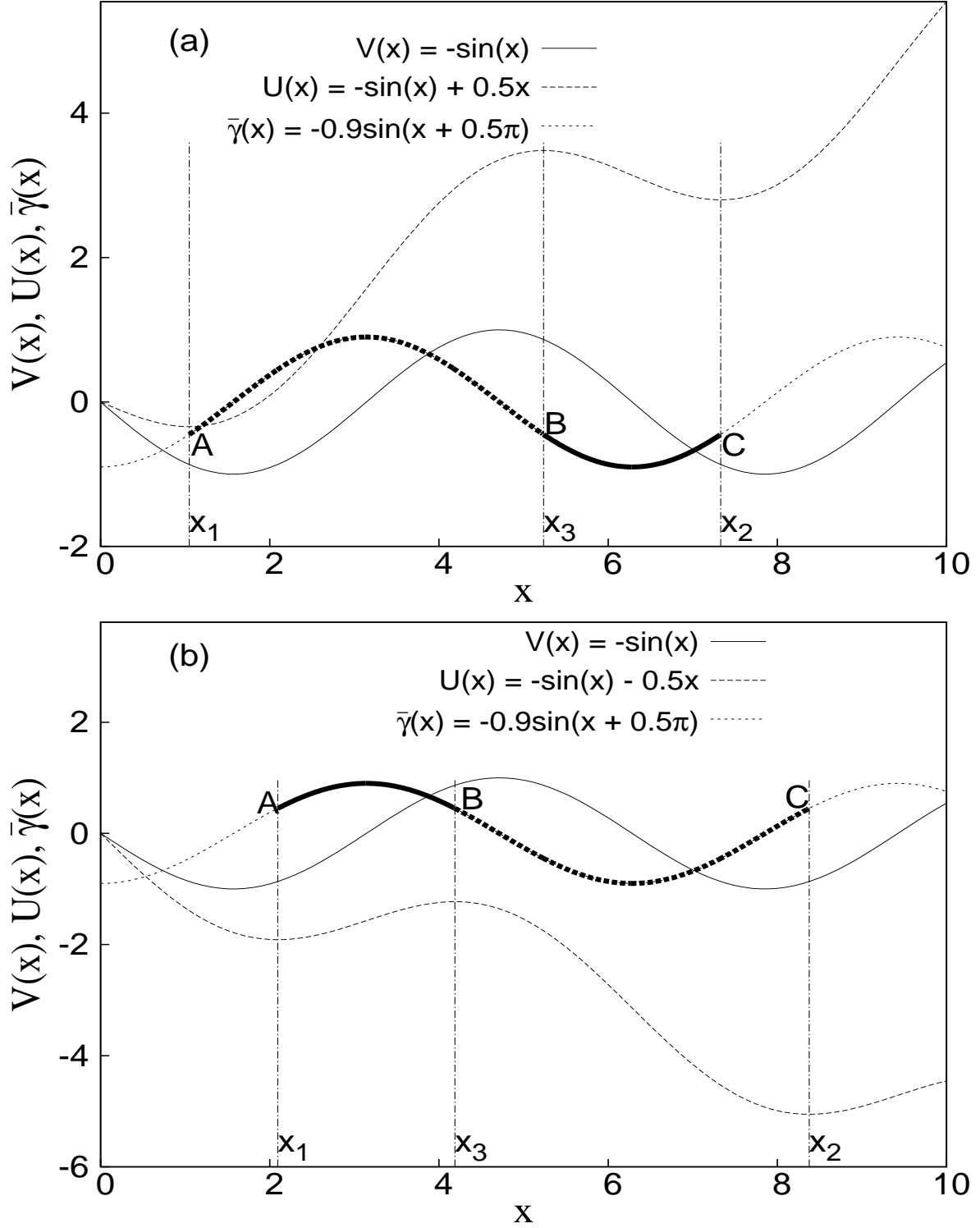


FIG. 1: The figure shows the variation of  $V(x), U(x), \bar{\gamma}(x)$  as a function of  $x$ . Here,  $\theta = 0.5\pi$ ,  $\lambda = 0.9$  with  $F_0 = -0.5$  in (a) and  $0.5$  in (b).

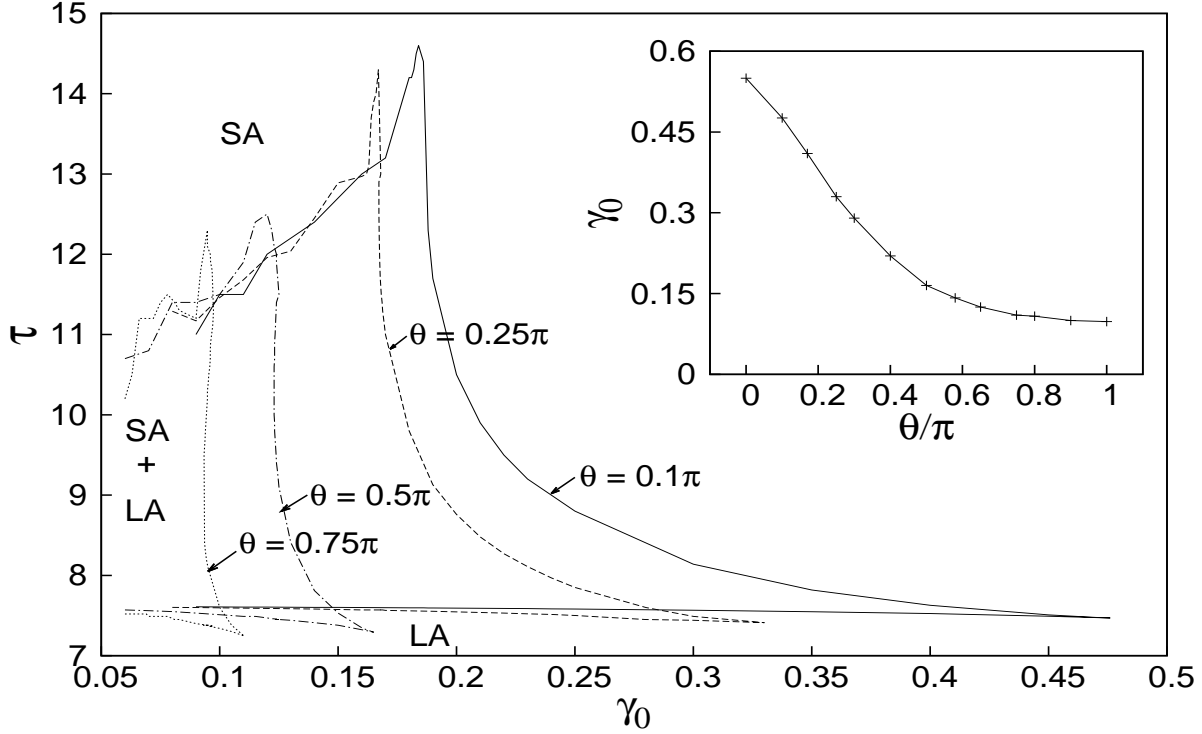


FIG. 2: The figure shows the boundaries of regions of coexistence of SA and LA states for  $\theta = 0.10\pi, 0.25\pi, 0.5\pi$  and  $0.75\pi$  at  $T = 0.000001$ . In the inset is plotted, for various  $\theta$ , the value of  $\gamma_0$  where the two dynamical states are not discernible.

the particle encounters a smaller barrier to surmount in the left direction with smaller mean friction (segment BC) and a larger barrier in the right direction with larger mean friction (segment AB). On the other hand in the latter case of Fig 1b the particle is to surmount the smaller barrier (of same height as in Fig. 1a) in the right direction but with a larger mean friction (segment AB) and the larger barrier in the left direction with a smaller mean friction (segment BC). Since the temperature is not large (typically  $< 0.2$ ) it is the smaller barrier that should contribute more to the displacement than the larger barrier and of course a smaller friction (and hence larger mobility) is more helpful in barrier crossing. Therefore one would expect a net current in the left direction when  $F(t) = F_0 \cos \omega t$  is considered over the entire period  $\tau = 2\pi/\omega$ . And this explains the net negative current observed in our numerical results to be described later for all  $0 < \theta < \pi$ . However, it is to be noted that the values of the parameters  $F_0$  and  $\gamma_0$  used here for illustration are to exaggerate the situation to bring the point home. In our work, in the following, we keep  $F_0 = 0.2$  and  $\gamma_0$  is varied but rarely so large as 1.0 used here. Yet the argument remains qualitatively valid. Can one

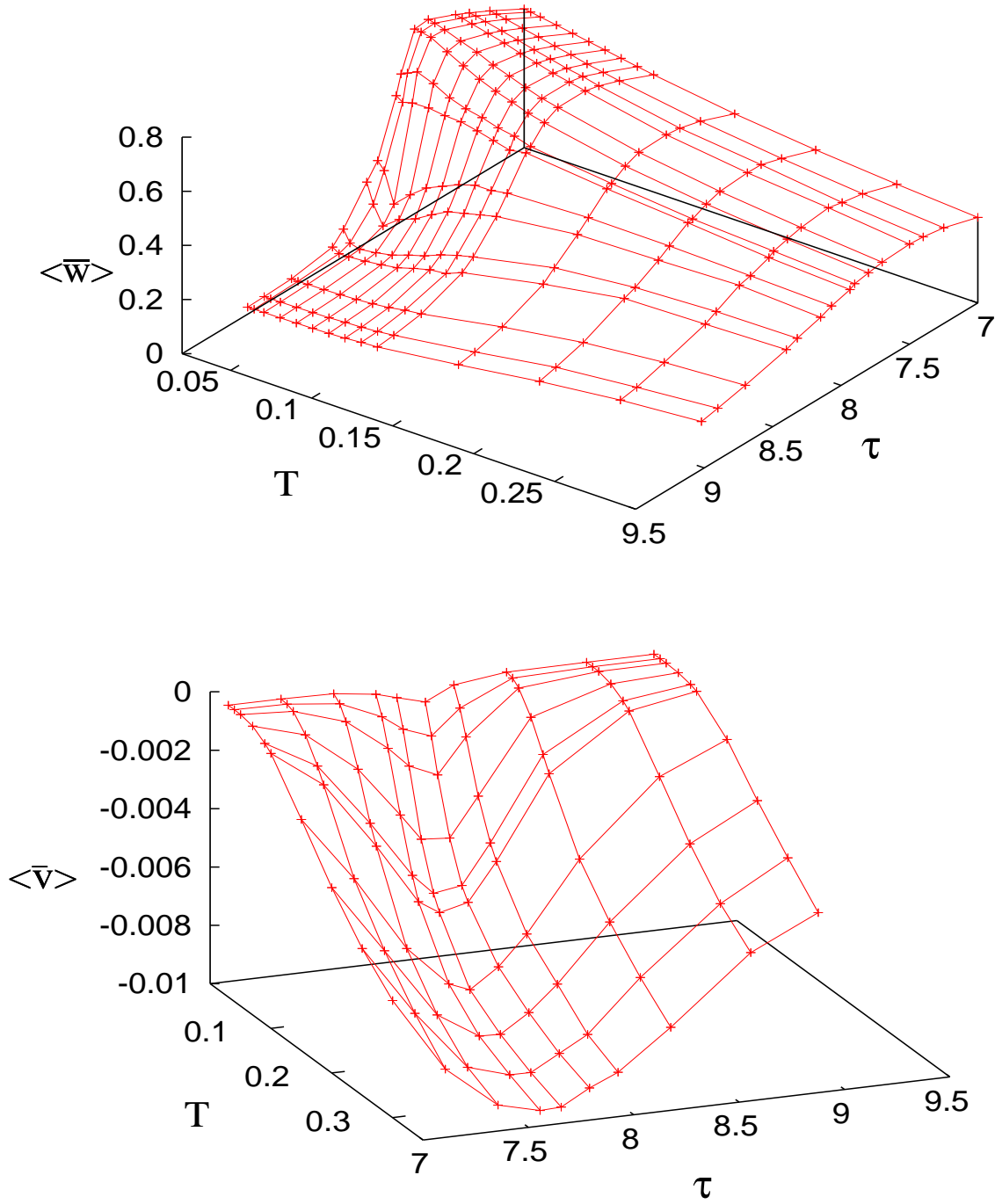


FIG. 3: The top figure shows the variation of  $\langle \bar{W} \rangle$  as a function of forcing period  $\tau$  and temperature  $T$ . Here  $\theta = 0.5\pi$ ,  $\lambda = 0.9$ ,  $F_0 = 0.2$  and  $\gamma_0 = 0.07$ . For the same set of parameter values, the bottom figure shows the variation of  $\langle \bar{v} \rangle$  as a function of forcing period  $\tau$  and temperature  $T$ .

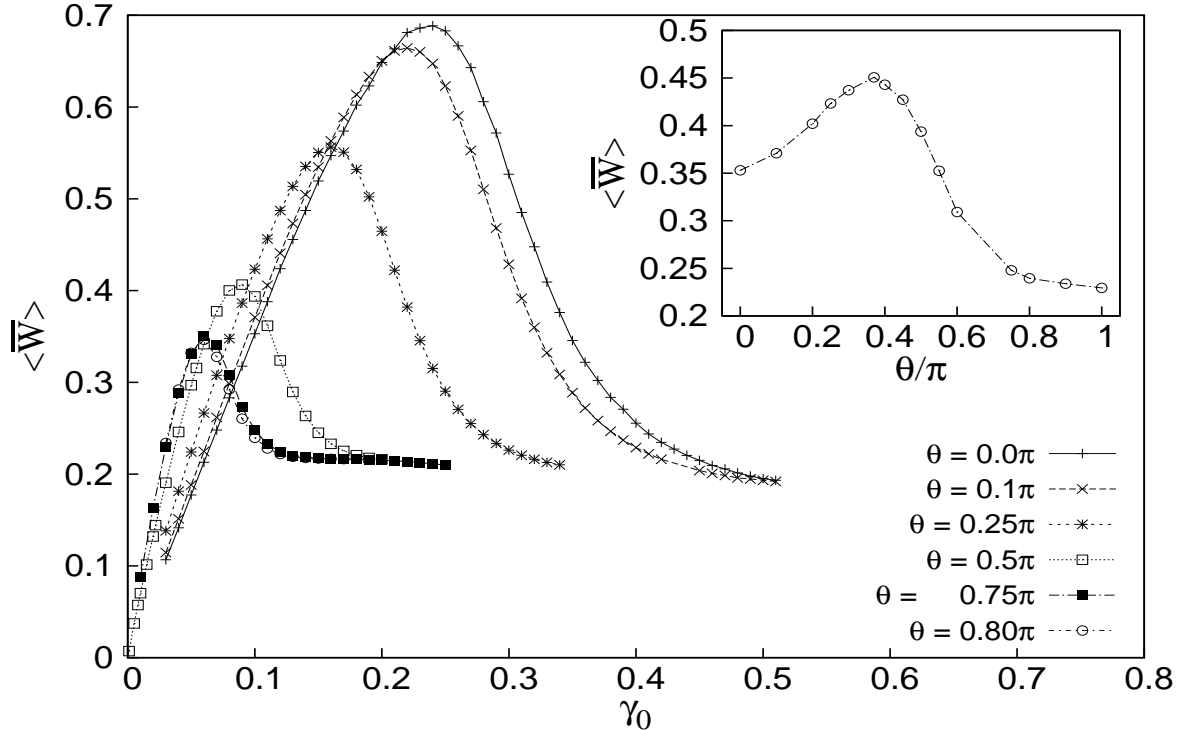


FIG. 4: The figure shows the variation of  $\langle \overline{W} \rangle$  as a function of  $\gamma_0$ . Here  $\lambda = 0.9$ ,  $F_0 = 0.2$ ,  $T = 0.1$  and  $\tau = 8.0$  for a set of  $\theta$  values as indicated in the plot. In the inset is shown the variation of  $\langle \overline{W} \rangle$  as a function of  $\theta$  for an *intermediate* value of  $\gamma_0 = 0.10$ , keeping other parameters same as that of the main plot.

extend this analogous argument to explain the magnitude of the net current too?

Of course, this situation can be brought out more effectively when the frictional asymmetry with respect to  $V(x)$  is maximum at  $\theta = 0.5\pi$  and thus one would expect the ratchet current to be the largest for  $\theta = 0.5\pi$ . However, frictional asymmetry is not the only factor that comes into play. A closer look at the nature of particle trajectories in the  $(\gamma_0 - \tau)$  space, as has been obtained previously is a similar system as in the present case, is quite educative in this respect.

### B. A brief summary of results from earlier works

At low temperatures the system shows two and only two kinds of particle trajectories,  $x(t)$ : a large amplitude trajectory (LA) with large phase lag with respect to  $F(t)$  and another with small amplitude (SA) and also small phase lag[38, 48, 49]. The two states of

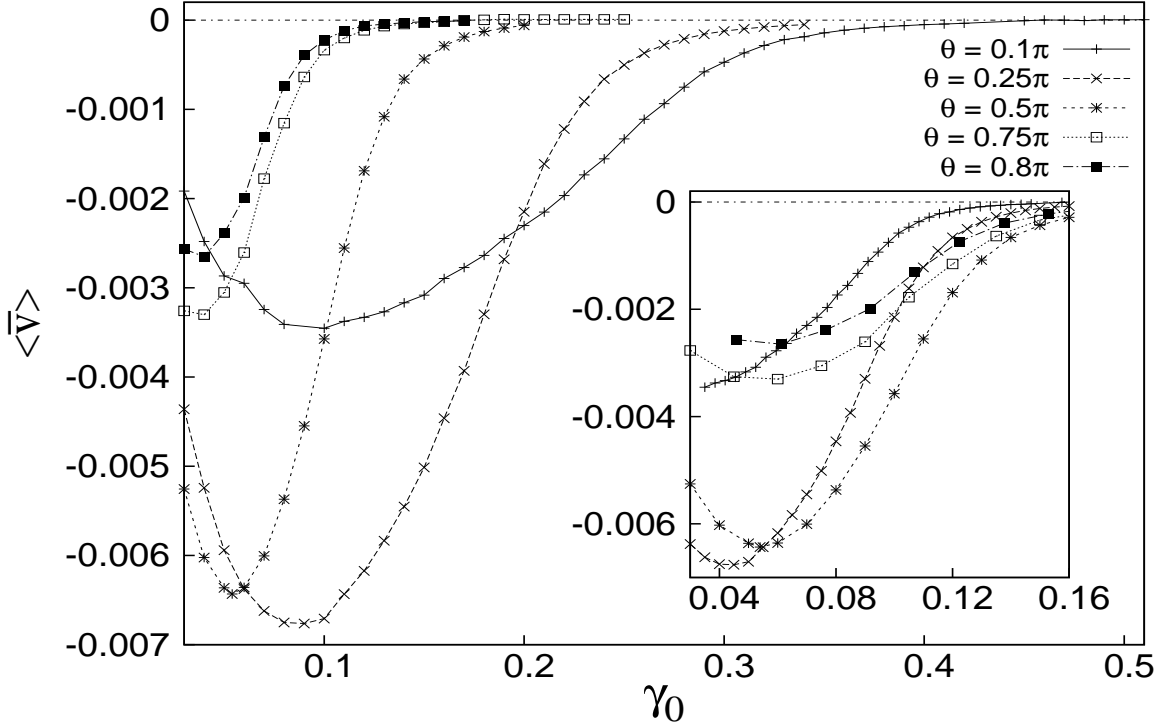


FIG. 5: The figure shows the variation of  $\langle \bar{v} \rangle$  as a function of  $\gamma_0$ . Here  $\lambda = 0.9$ ,  $F_0 = 0.2$ ,  $T = 0.1$  and  $\tau = 8.0$  for a set of  $\theta$  values as indicated in the plot. In the inset is shown the same plot but after a suitable scaling factor (different for different  $\theta$ , see text) is applied to the abscissa.

trajectories occur in a restricted range of parameter space  $(\gamma, \omega)$ . In particular  $\omega$  should be close to the natural frequency of oscillation ( $\omega \approx 1$ ) at the bottom of the potential. This frequency ( $\omega \approx 1$ ) is much larger (about  $10^2$  times) than the mean rate of passage across the potential barrier. The occurrence of these trajectories depends on the initial conditions of position  $x(t=0)$  (within a period of  $V(x)$ ) and velocity  $v(t=0)$  (Here we choose  $v(0) = 0$ ). Figure 2 is an extension of Fig. 7 of Ref.[38] showing the region of coexistence of these two ‘dynamical states’ of trajectories in the  $(\gamma_0 - \tau)$  plane. The nature of the curves for various  $\theta$  values clearly suggests that the effectiveness of  $\gamma_0$  decreases as  $\theta$  is decreased[38]. This can also be seen from Fig 1a that when, for example,  $\theta = 0$  ( $\pi$ ) the particle encounters the least (largest) average friction while having its motion about the bottom of the potential. The value of  $\gamma_0$  at which the region of coexistence of the two states of trajectories vanishes may roughly be taken as the reciprocal measure of an effective  $\gamma_0$  for a given  $\theta$ . In the inset of Fig.2 are plotted the  $\gamma_0$  values at which the regions of coexistence just vanish. When the friction becomes less effective (smaller  $\theta$ ) the net particle current may be larger than

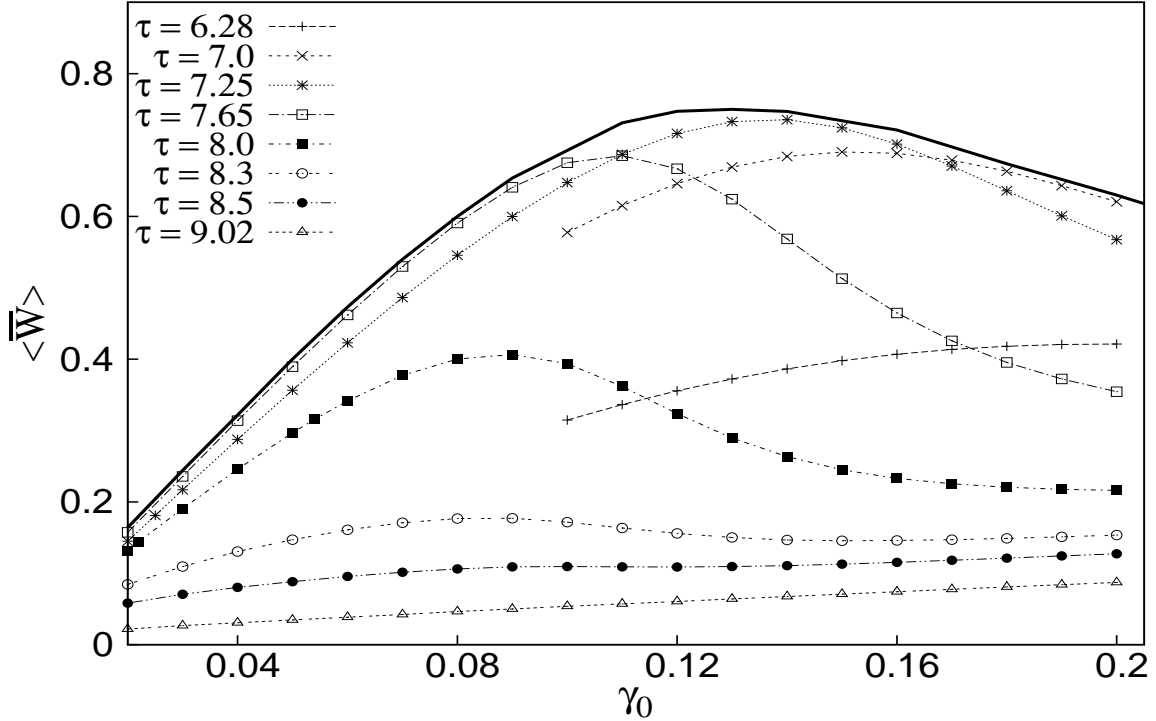


FIG. 6: The figure shows the variation of  $\langle \overline{W} \rangle$  as a function of  $\gamma_0$ . Here  $\lambda = 0.9$ ,  $F_0 = 0.2$ ,  $T = 0.1$  and  $\theta = 0.5\pi$  for a set of  $\tau$  values as indicated in the plot. The thick line however denotes the maximum  $\langle \overline{W} \rangle$ , which occurs for different driving frequencies  $\omega$ , as a function of  $\gamma_0$ .

when the friction becomes more effective (larger of  $\theta$  in the range  $0 < \theta < \pi$ ). Thus the frictional asymmetry plays a dual role as far as the magnitude of the net (ratchet) current is concerned.

We confine our work mostly in the region of coexistence of the two dynamical states for we expect to get interesting results in this region. In particular, it has been shown that the energy of dissipation of the system per period  $\tau$  of  $F(t)$  shows a maximum at an intermediate noise strength (or temperature  $T$ ). Or, equivalently, the ratio of the output signal to input noise peaks as a function of temperature for a given  $\tau$ ,  $\gamma_0$ , and small  $F_0$ . This important phenomenon is termed as stochastic resonance. Stochastic resonance is usually observed in bistable systems at a frequency of the order of the mean rate of passage across the barrier. However, in this case it refers to the sinusoidal potential  $U(x)$ . The energy dissipation or the input energy plays a key role in the efficiency calculation of the frictional ratchet as will be discussed in the subsequent sections. The input energy (and ratchet currents) were calculated earlier in the  $(\tau - T)$  plane[38]. The results are summarized in Fig.3.

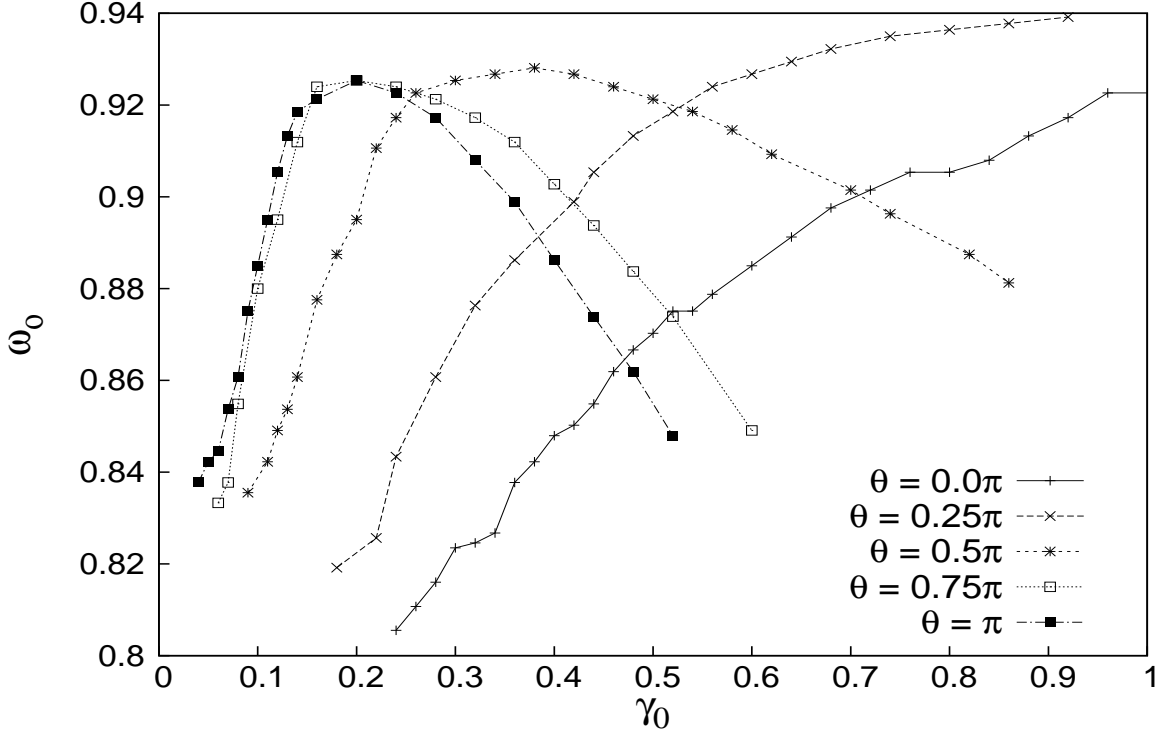


FIG. 7: The figure shows the conventional resonance frequency  $\omega_0$  as a function of  $\gamma_0$ . Here  $\lambda = 0.9$ ,  $F_0 = 0.2$  and  $T = 0.1$  for a set of  $\theta$  values as indicated in the plot.

#### IV. NUMERICAL RESULTS

In the present numerical work, we take  $N = 200000$  cycles of the drive to obtain the necessary ratchet currents. We calculate the difference  $(x(t = N\tau) - x(t = 0))$  for each initial condition used to calculate  $\bar{v} = \frac{(x(t=N\tau) - x(t=0))}{N\tau}$ . The deviations of these  $\bar{v}$  from the mean  $\langle \bar{v} \rangle$  is calculated as an ensemble average over all trajectories whose initial positions are uniformly distributed within a period of the potential. One can then obtain the necessary standard deviations  $\Delta v$  to form the error bars.

##### A. Input energy and ratchet current

We explore the behavior of net (ratchet) current,  $\langle \bar{v} \rangle$ , as well as the input energy,  $\langle \bar{W} \rangle$ , as a function of  $\gamma_0$  for various values of  $\theta$  and  $\tau$ . From symmetry arguments  $\langle \bar{v} \rangle = 0$  for  $\theta = 0, n\pi$  for all integral  $n$ . Also, as it should,  $\pi \leq \theta < 2\pi$  gives the same information about  $\langle \bar{v} \rangle$  as in case of  $0 \leq \theta < \pi$ , for any value of  $\gamma_0$ ,  $\lambda$  and  $\tau$ , only the direction is reversed. Note that we keep the amplitude  $F_0$  of the drive  $F(t)$  fixed and equal

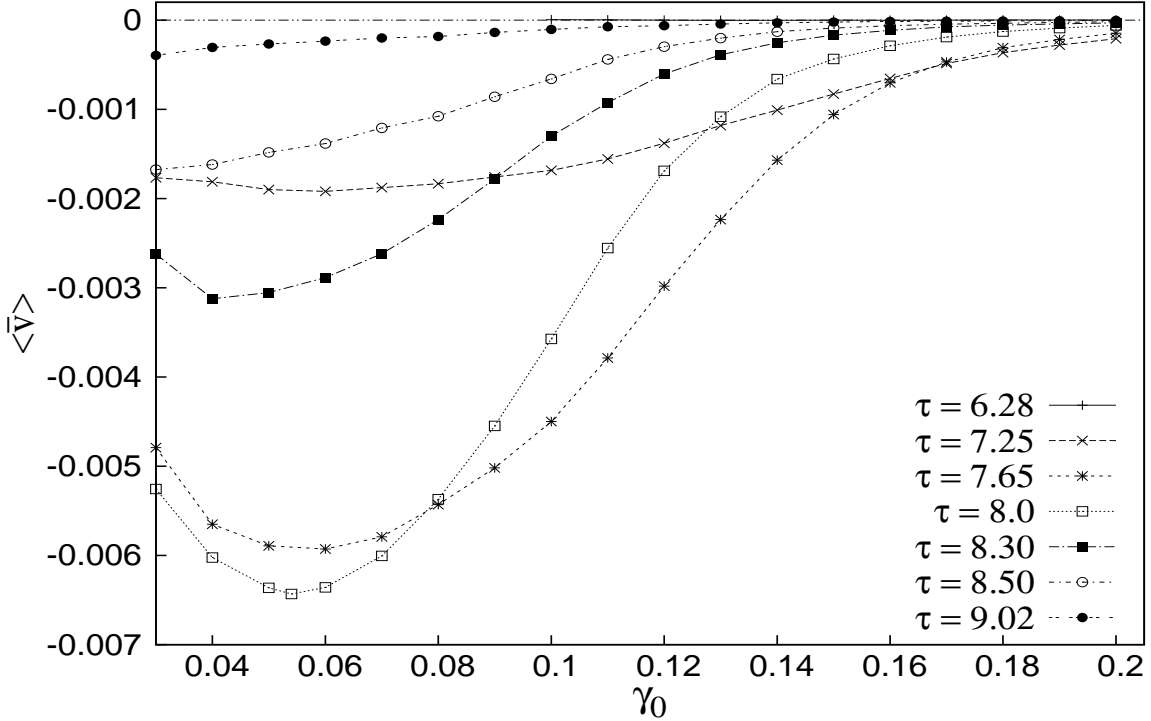


FIG. 8: The figure shows the variation of  $\langle \bar{v} \rangle$  as a function of  $\gamma_0$ . Here  $\lambda = 0.9$ ,  $F_0 = 0.2$ ,  $T = 0.1$  and  $\theta = 0.5\pi$  for a set of  $\tau$  values as indicated in the plot.

to 0.2. Though  $\langle \bar{v} \rangle = 0$  for  $\theta = 0, \pi$ , the input energy  $\langle \bar{W} \rangle \neq 0$ . Figure 4 shows  $\langle \bar{W} \rangle$  as a function of  $\gamma_0$  at a constant temperature  $T = 0.1$  and  $\tau = 8.0$  for various values of  $\theta$ . Interestingly, for small  $\gamma_0 < \gamma_{01}$  ( $\gamma_{01} \approx 0.05$ ) and for large  $\gamma_0 > \gamma_{02}$  ( $\gamma_{02} \approx 0.2$ ),  $\langle \bar{W} \rangle(\theta)$  shows monotonic (respectively, increasing and decreasing) behavior for fixed  $\gamma_0$ . However, in the intermediate range of  $\gamma_{01} \leq \gamma_0 \leq \gamma_{02}$ ,  $\langle \bar{W} \rangle(\theta)$  shows peaking behavior. The width of the intermediate range of  $\gamma_0$  depends on  $\tau$ , etc. It is roughly in this intermediate range where the phenomenon of stochastic resonance (peaking of  $\langle \bar{W} \rangle$  as a function of temperature for fixed  $\gamma_0, \theta, F_0$  and  $\tau$ ) is obtained. In the inset of Fig. 4,  $\langle \bar{W} \rangle(\theta)$  is shown for one of such intermediate value of  $\gamma_0 = 0.10$  which displays the described peaking behaviour.

In Fig. 5 is shown the ratchet current  $\langle \bar{v} \rangle$  as a function of  $\gamma_0$  for various values of  $\theta$  with other parameters fixed as in Fig. 4. Note that particle trajectory properties (including the hysteresis loops) for  $\theta = 0.5\pi$  are closest to the properties of that of a system with uniform friction with  $\lambda = 0$  (see Fig. 5 of Ref.[38]). As mentioned earlier,  $\theta = 0.5\pi$  provides the largest left-right asymmetry due to frictional nonuniformity and hence one would expect

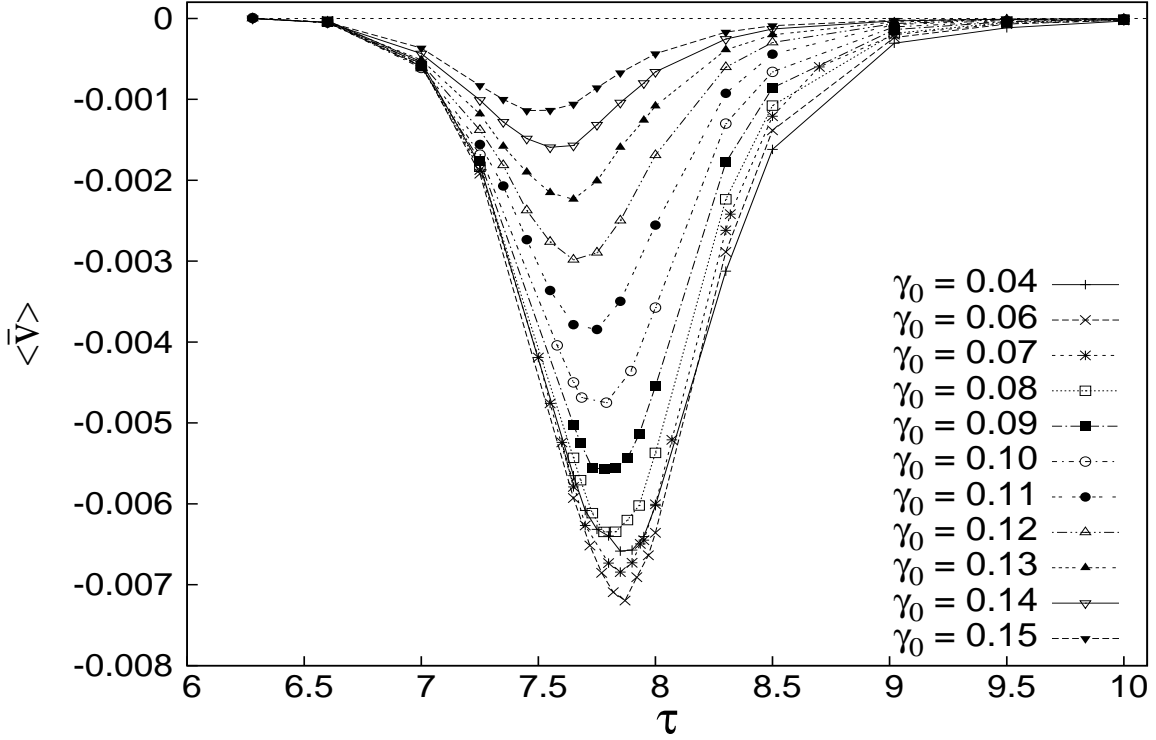


FIG. 9: The figure shows the variation of  $\langle \bar{v} \rangle$  as a function of  $\tau$ . Here  $\lambda = 0.9$ ,  $F_0 = 0.2$ ,  $\theta = 0.5\pi$  and  $T = 0.1$  for a set of  $\gamma_0$  values as indicated in the plot.

to obtain largest  $\langle \bar{v} \rangle$  for  $\theta = 0.5\pi$ . However, Fig. 5 shows that for  $\gamma_0 \geq 0.05$ , the mean velocity  $\langle \bar{v} \rangle$  are larger for  $\theta < 0.5\pi$  than  $\langle \bar{v} \rangle$  for  $\theta = 0.5\pi$ .

The above apparent anomaly can be explained by the suggestion that  $\langle \bar{v} \rangle$  is due to the combined effect of frictional asymmetry and effective value  $\bar{\gamma}_0$  of  $\gamma_0$ . The inset of Fig. 2 gives an idea that as  $\theta$  decreases from  $0.5\pi$ ,  $\bar{\gamma}_0$  decreases and it gets enhanced  $\bar{\gamma}_0$  for  $\theta > 0.5\pi$ . For example, in Fig. 2, the region of coexistence of the dynamical states of trajectories closes at  $\gamma_0 = 0.165$  for  $\theta = 0.5\pi$  and for  $\theta = 0.25\pi$  and  $0.75\pi$  the regions close respectively at  $\gamma_0 = 0.33$  and  $0.11$ . If we rescale the abscissa of Fig. 5 accordingly, for example by a factor of  $\frac{0.165}{0.33}$  for  $\theta = 0.25\pi$ , what results is shown in the inset of Fig. 5. It too, however, does not entirely isolate the two effects, as can be inferred from the inset; one should change the value of  $\langle \bar{v} \rangle$  as well, for example by a factor of, say,  $0.7$ . But, of course, we have no basis to arrive at the said factor. The message of Fig. 5, therefore, remains that  $\langle \bar{v} \rangle$ , unlike  $\langle \bar{W}(\theta) \rangle$ , shows nonmonotonic behavior as a function of  $\theta$  at fixed  $\gamma_0$  all through the abscissa of Fig. 5.

Figure 6 gives the plot of  $\langle \bar{W} \rangle$  as a function of  $\gamma_0$  for  $\theta = 0.5\pi$  for various values of the

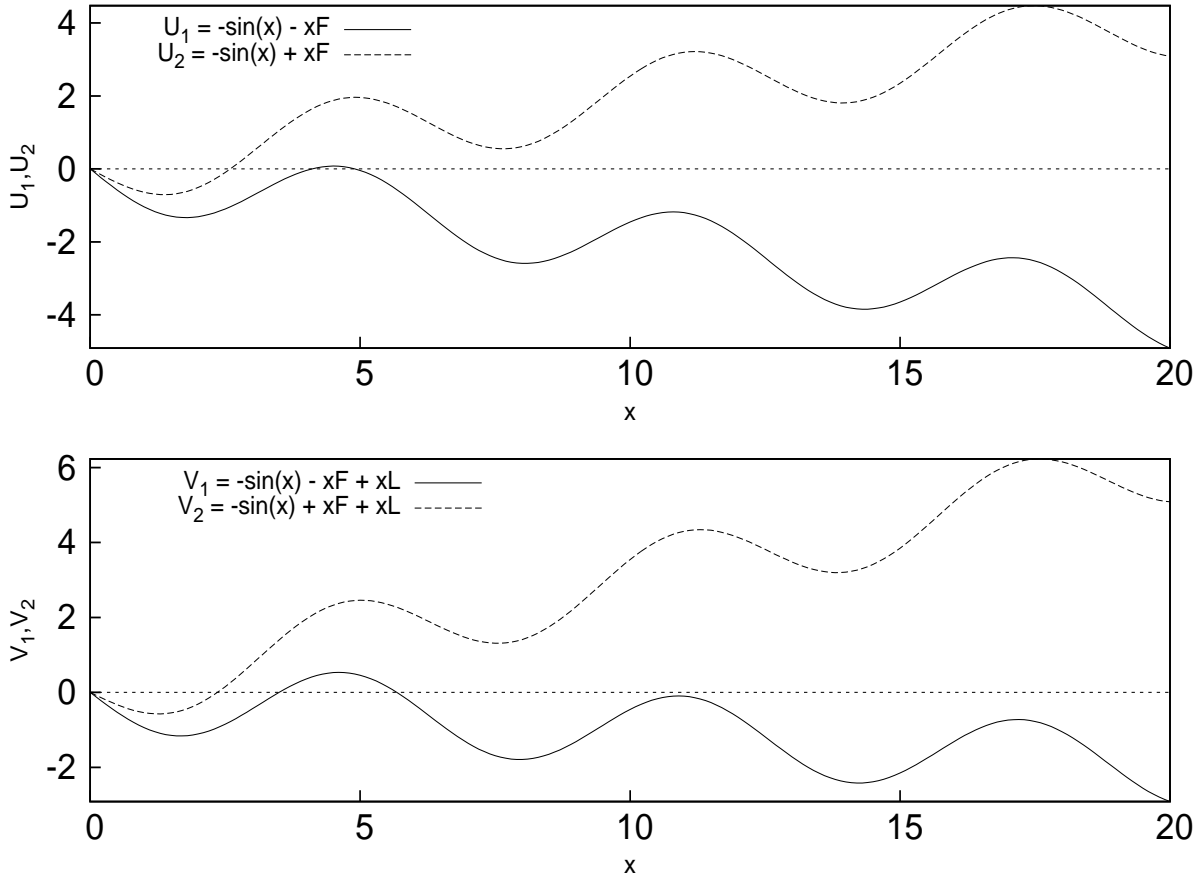


FIG. 10: The panels shows the effect of the forcing on the potential. At the top panel is shown (in the absence of load)  $U_1$  as the effective potential at the beginning of the forcing period whereas  $U_2$  is the effective potential at half-period of the forcing. The bottom panel shows the effect of the forcing on the potential when a load is present. This is the so called washboard potential.  $V_1$  is the effective potential at the beginning of the forcing period whereas  $V_2$  is the effective potential at half-period of the forcing.

period  $\tau$  of the applied field  $F(t)$  at  $T = 0.1$ . For other  $\theta$  values the graph will have similar qualitative character. We have chosen  $\theta = 0.5\pi$  because it provides the largest asymmetry in addition to  $\overline{\gamma_0}$  being equal to  $\gamma_0$ . From the graph it is clear that for all values of  $\gamma_0$ , the input energy  $\langle \overline{W} \rangle$  shows peaking behaviour as a function of the period  $\tau$ . However, the value of  $\tau$ , say,  $\tau_0$ , at which  $\langle \overline{W} \rangle$  peaks for a given value of  $\gamma_0$  changes. The dark curve in Fig. 6 is the envelope of  $\langle \overline{W} \rangle$  giving the largest possible  $\langle \overline{W} \rangle$  ( $\gamma_0$ ). For example at  $\gamma_0 = 0.11$ ,  $\langle \overline{W} \rangle$  becomes largest for  $\tau = \tau_0 = 7.4$ , etc. Since  $\langle \overline{W} \rangle$  is equal to the hysteresis loop area it gives the mean energy absorbed per cycle of  $F(t)$ . Thus,  $\tau_0$  can

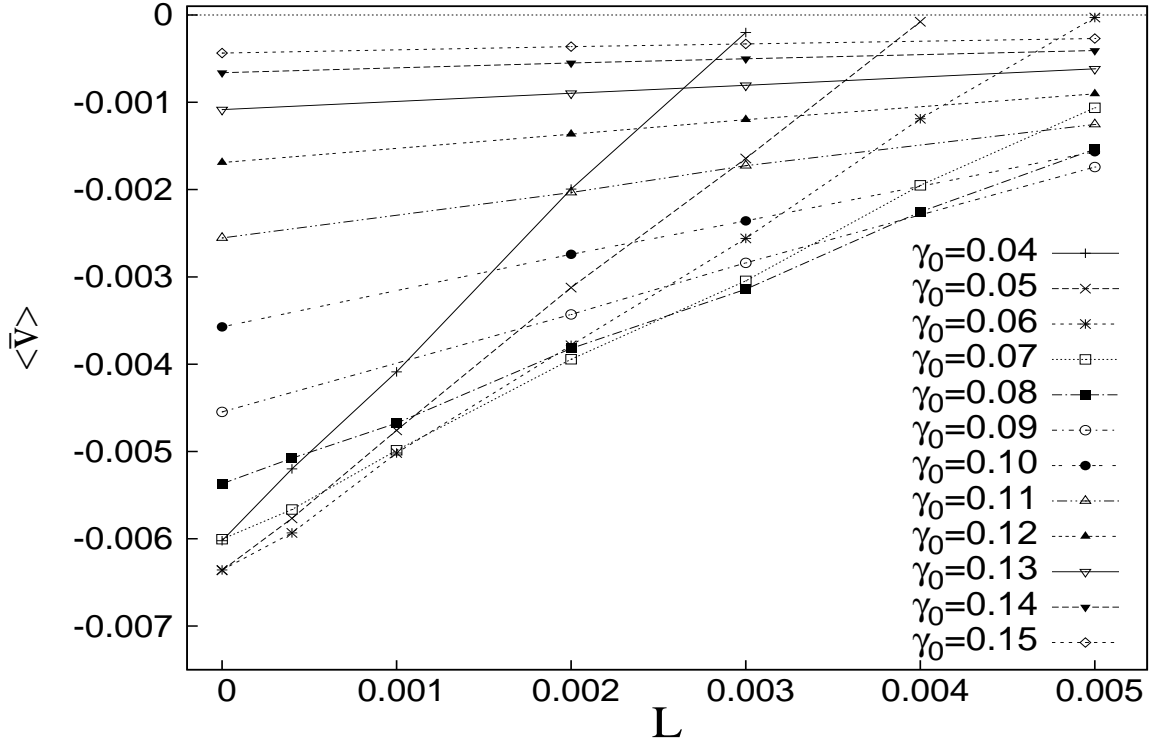


FIG. 11: The figure shows the variation of  $\langle \bar{v} \rangle$  as a function of load  $L$  for a set of  $\gamma_0$  values as indicated in the graph. Here  $\lambda = 0.9$ ,  $F_0 = 0.2$ ,  $\theta = 0.5\pi$ ,  $T = 0.1$  and  $\tau = 8.0$ . The top most horizontal line is the zero line.

be considered as the period of conventional resonance at the given mean damping  $\gamma_0$ . The corresponding resonance frequencies  $\omega_0 = \frac{2\pi}{\tau_0}$  are plotted as a function of  $\gamma_0$  in Fig. 7 for various values of  $\theta$ . The curves show how damping affects the conventional resonance in a sinusoidal potential, as opposed to in the usual limit of a parabolic potential. In particular, the curve for  $\theta = 0.5\pi$  provides important information about variation of resonance frequency, for example, of a driven damped (large amplitude) pendulum as a function of damping.

From the figure (Fig. 7) it is clear that the conventional resonance frequency in a sinusoidal potential peaks at an intermediate value of  $\gamma_0 = \gamma_0^{peak}$ . The value of  $\gamma_0^{peak}$  increases with decreasing value of  $\theta$ . At this temperature ( $T = 0.1$ ) the numerical results become less precise for smaller  $\theta$  values. Also, one would expect all curves to converge at a common value of resonance frequency  $\omega_0$  for all values of  $\theta$  at  $\gamma_0 = 0$ . However, in our numerical work it is hard to obtain the conventional resonance at low  $\gamma_0$  values with small error bars. That is why we have not shown the complete graphs in the lower region of  $\gamma_0$ . Also, for smaller  $\theta$  values (e.g.,  $\theta = 0$  and  $0.25\pi$ ) the larger  $\gamma_0$  region beyond  $\gamma_0 = 1$  is not explored.

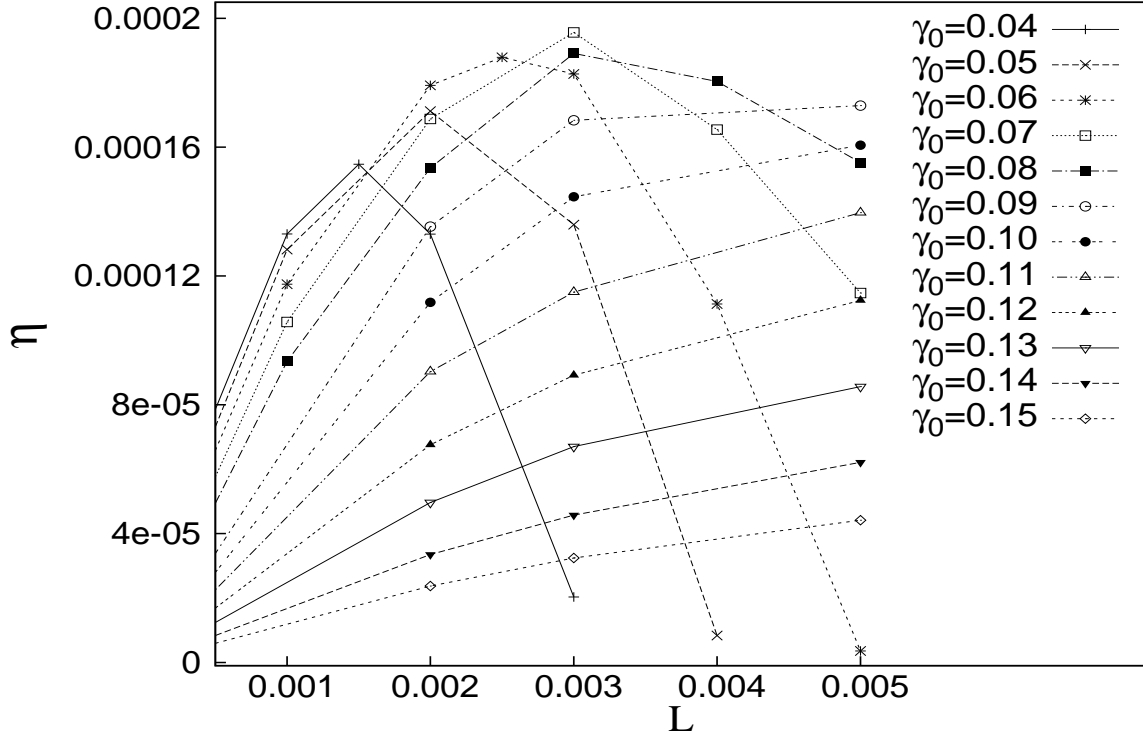


FIG. 12: The figure shows the variation of  $\eta$  as a function of load  $L$  for a set of  $\gamma_0$  values as indicated in the graph. Here  $\lambda = 0.9$ ,  $F_0 = 0.2$ ,  $\theta = 0.5\pi$ ,  $T = 0.1$  and  $\tau = 8.0$ .

In Fig. 8 is plotted  $\langle \bar{v} \rangle$  as a function of  $\gamma_0$  for  $\theta = 0.5\pi$  and various values of  $\tau$  as in Fig. 6.  $\langle \bar{v} \rangle$  vanishes for  $\gamma_0 = 0$  for all  $\tau$  and becomes very small for large  $\gamma_0$  values and hence peaks at intermediate  $\gamma_0$  values. From the graphs it is also clear that  $\langle \bar{v} \rangle$  shows nonmonotonic behaviour as a function of  $\tau$  for fixed values of  $\gamma_0$  in the entire range of abscissa. Figure 9 summarizes  $\langle \bar{v} \rangle (\tau)$  for various  $\gamma_0$  values. Interestingly, the graphs show that appreciable ratchet current  $\langle \bar{v} \rangle$  can be obtained only in a limited range of  $\tau$  values, roughly  $6.5 \leq \tau \leq 9.5$ , for all values of  $\gamma_0$ . Note that this is roughly the domain of parameter space ( $\gamma_0 - \tau$ ) where stochastic resonance is expected to occur in sinusoidal potentials. Just as the period of conventional resonance, the value of  $\tau$  at which  $\langle \bar{v} \rangle$  peaks decreases with increase of  $\gamma_0$ . Although interesting, we cannot ascribe any physical significance to this behaviour unlike in the previous case of conventional resonance.

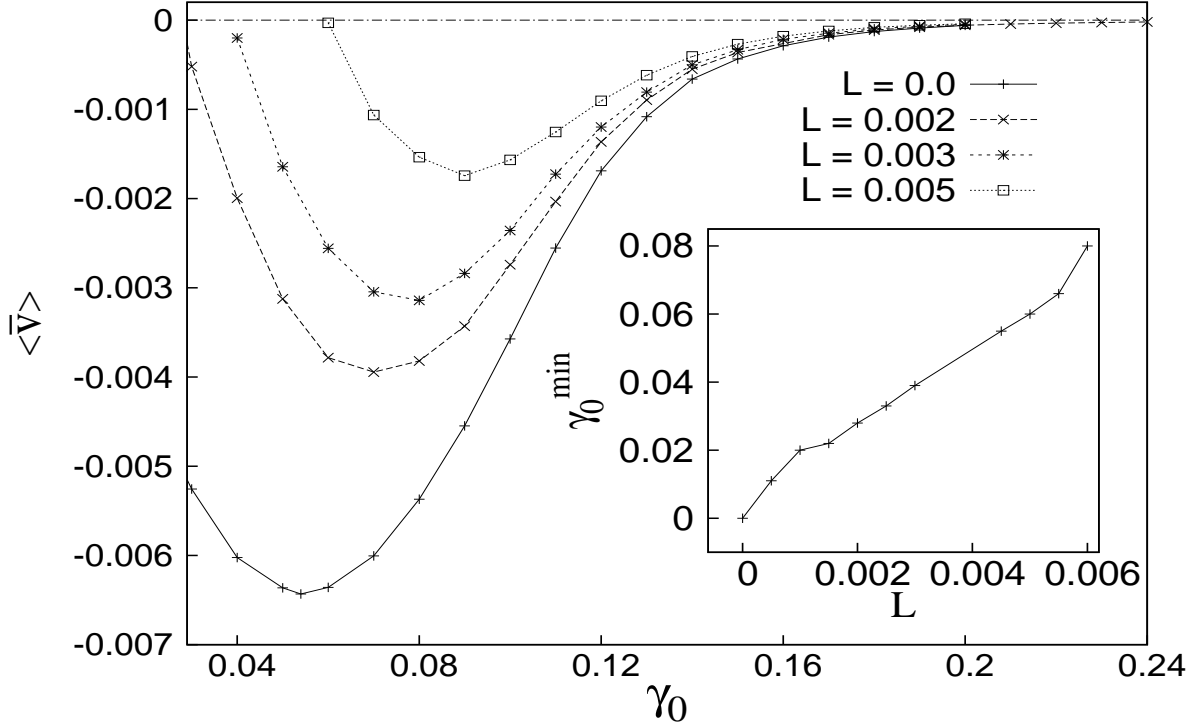


FIG. 13: The figure shows the variation of  $\langle \bar{v} \rangle$  as a function of  $\gamma_0$  for the load-free case and also for a set of load,  $L$ , values as indicated in the plot. Here  $\lambda = 0.9$ ,  $F_0 = 0.2$ ,  $\theta = 0.5\pi$ ,  $T = 0.1$  and  $\tau = 8$ . In the inset is calculated the maximum  $\gamma_0 = \gamma_0^{\min}$  where work can still be obtained by the ratchet as a function of load  $L$ .

### B. Ratchet current against applied load

We now study the behavior of ratchet current  $\langle \bar{v} \rangle$  by applying a load  $L$  opposing the current  $\langle \bar{v} \rangle$ . Since the numerically obtained current  $\langle \bar{v} \rangle$  is negative, we apply  $L$  such as to tilt the potential with negative slope to oppose the current without load. This essentially means that the particle is now subjected to the washboard potential  $V(x) = -\sin(x) + xL$ , whose average value over one period is in the direction of the load. This modifies the equation of motion as given below.

$$\frac{d^2x}{dt^2} = -\gamma(x)\frac{dx}{dt} - \frac{\partial V(x)}{\partial x} + F(t) + L + \sqrt{\gamma(x)T}\xi(t), \quad (4.1)$$

with  $L > 0$ . We define the thermodynamic efficiency of the ratchet as

$$\eta = \frac{L \langle \bar{v} \rangle}{\langle \bar{W} \rangle / \tau + L \langle \bar{v} \rangle}. \quad (4.2)$$

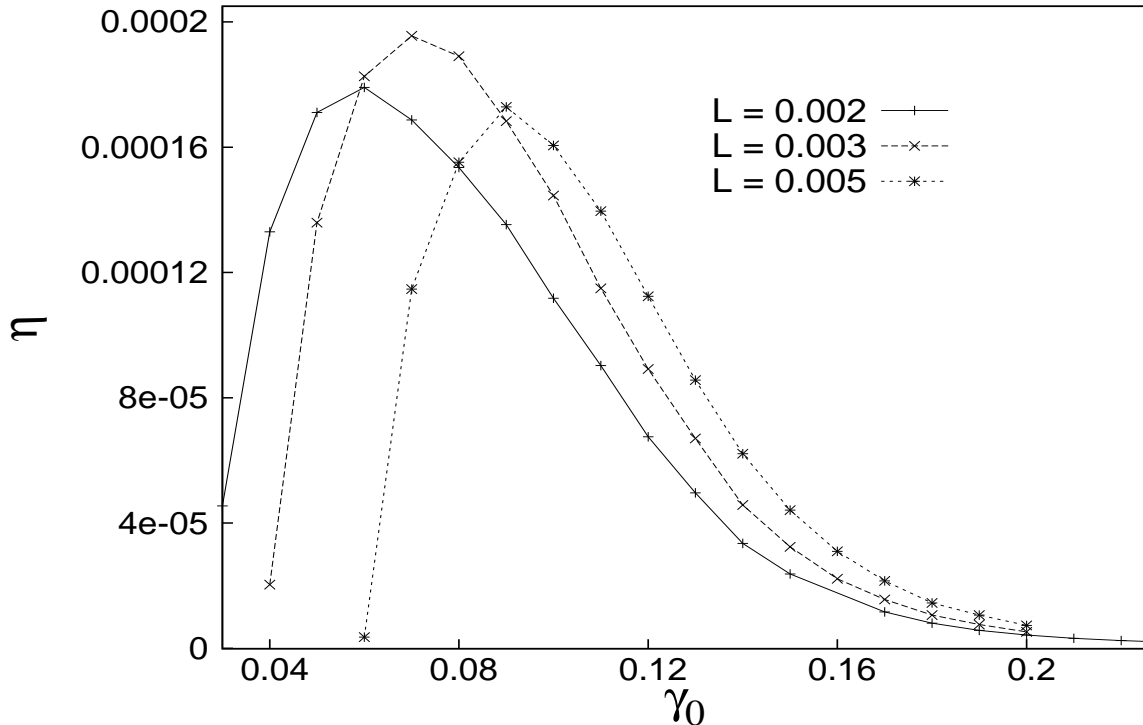


FIG. 14: The figure shows the variation of  $\eta$  as a function of  $\gamma_0$  for the set of load,  $L$ , values as indicated in the plot. Here  $\lambda = 0.9$ ,  $F_0 = 0.2$ ,  $\theta = 0.5\pi$ ,  $T = 0.1$  and  $\tau = 8$ .

Here, we use the natural definition of efficiency as the ratio of work done by the signal,  $F(t)$ , against the load  $L$  and the total energy spent in order to extract that work.

We note that  $\langle \overline{W} \rangle$  is independent of the load  $L$  because Eq. (2.10) is true for each and every trajectory, that is, the mean absorbed energy in the presence of load would be the same as in the load-free case because  $W(0, N\tau)$  depends only on the explicit time dependence of  $U(x, t)$  through  $F(t)$ . We provide below a brief plausible physical explanation on the independence of  $\overline{W}$  on  $L$ , to add to the mathematical equality of Eq. (2.10).

The top panel of Fig. 10 shows the effective potential  $U(x) = -\sin(x) + xF(t)$  with  $F(t) = F_0 \cos(\omega t)$  for the two extreme values of  $F(t)$ , that is, when  $F(t) = F_0$ :  $U(x) = U_1$ , and when  $F(t) = -F_0$ :  $U(x) = U_2$ . We draw a line corresponding to  $U(x) = 0$  for reference. At the two extreme values of  $F(t)$ ,  $U_1$  and  $U_2$  are tilted with equal slope but in opposite directions. If the friction offered by the medium is taken to be uniform, the mean velocities of the particle are equal in magnitude in both extreme instances of the forcing owing to identical trajectories  $x(t)$ . Hence, work done on the system by the external forcing and hence the energy dissipated by the system in the two cases are the same. Now let us

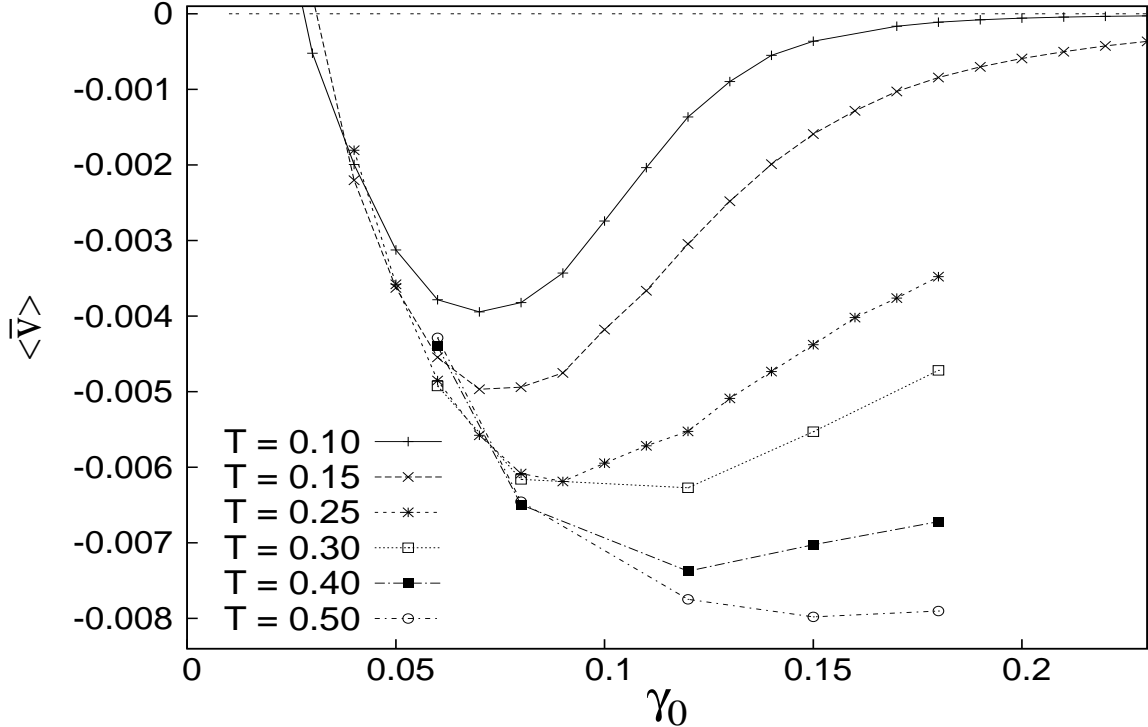


FIG. 15: The figure shows the variation of  $\langle \bar{v} \rangle$  as a function of  $\gamma_0$  for various  $T$  values as indicated in the graph for constant load  $L = 0.002$  and  $\tau = 8$ . Here  $\lambda = 0.9$ ,  $F_0 = 0.2$  and  $\theta = 0.5\pi$

consider the situation when, in addition, an external load  $L$  is applied to the system. The bottom panel of Fig. 10 shows the potential profiles ( $V_1$  and  $V_2$ ) in the two extreme cases as considered earlier. Clearly, the mean velocities in the two situations are unequal: one larger than in case of  $U_1$ , for example, and the other smaller. This amounts to a mean energy dissipation per cycle of  $F(t)$  nearly the same as in the earlier case of  $L = 0$ .

In Fig. 11, we plot  $\langle \bar{v} \rangle$  as a function of  $L$  for various values of  $\gamma_0$  for  $T = 0.1$ ,  $\theta = 0.5\pi$ , and  $\tau = 8.0$ . We continue to increase the load  $L$  so long as  $\langle \bar{v} \rangle$  continues to be in the same direction as when  $L = 0$ , that is as long as the system does work against the load. The variation of  $\langle \bar{v} \rangle$  as a function of  $\gamma_0$  at  $L = 0$  for various  $\tau$  values are shown to be nonmonotonic in Fig. 8. The  $\langle \bar{v} \rangle (L)$  curves appear to be almost straight lines with their slopes gradually decreasing with increasing  $\gamma_0$  values and their intercepts at  $L = 0$  as suggested by Fig. 8. Thus, for large  $\gamma_0$  values, for example  $\gamma_0 = 0.15$ , the curves run almost parallel to the abscissae and hence a large load can be applied without  $\langle \bar{v} \rangle$  reversing its direction. On the other hand, for smaller values of  $\gamma_0$ , only a small load can be applied.

The changing 'slope' of  $\langle \bar{v} \rangle (L)$  for various  $\gamma_0$  have a another curious fallout too. For

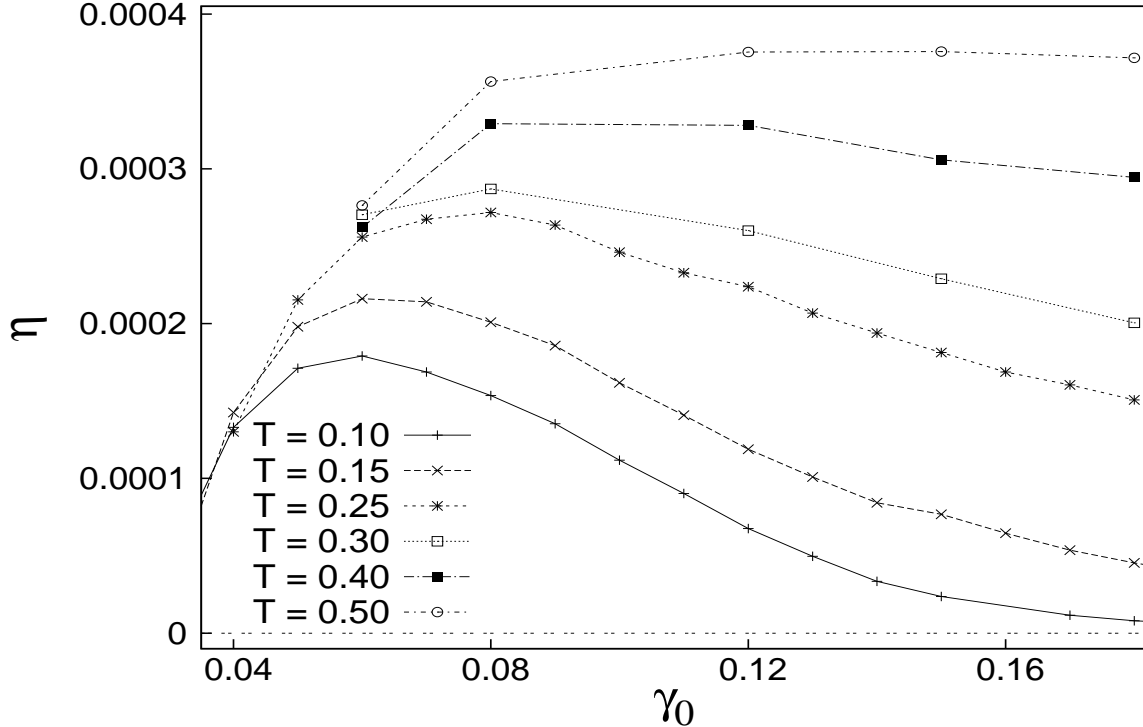


FIG. 16: The figure shows the variation of  $\eta$  as a function of  $\gamma_0$  for various  $T$  values (as indicated in the bottom left region of the graph) for constant load  $L = 0.002$  and  $\tau = 8$ . Here  $\lambda = 0.9$ ,  $F_0 = 0.2$  and  $\theta = 0.5\pi$ .

example, though at  $L = 0$ ,  $\langle \bar{v} \rangle$  for  $\gamma_0 = 0.04$  is larger than  $\langle \bar{v} \rangle$  for  $\gamma_0 = 0.08$ , as the load is increased beyond a certain value,  $\langle \bar{v} \rangle$  for  $\gamma_0 = 0.08$  becomes larger than for  $\gamma_0 = 0.04$ . And this acquired inequality continues to remain so over a large range of  $L$ . It is very appropriate to ask, therefore, whether the ratchet becomes more efficient for  $\gamma_0 = 0.08$  than for  $\gamma_0 = 0.04$  for the same applied load. And, of course, whether this trend is true for other  $\gamma_0$  values as well as suggested by Fig. 11?

Figure 12 shows the corresponding efficiencies,  $\eta$ . It shows that  $\eta$  is a nonmonotonic function of  $L$  and  $\eta$  peaks at larger value of  $L$  for larger  $\gamma_0$ . At lower loads smaller  $\gamma_0$  ratchets are more efficient than larger  $\gamma_0$  ratchets even though the current  $\langle \bar{v} \rangle$  is a nonmonotonic function of  $\gamma_0$  when  $L = 0$ . However, for larger  $L$ , ratchets with larger  $\gamma_0$  are more efficient than ratchets with smaller  $\gamma_0$ . This interesting result can, however, be roughly understood by considering the behaviour of both  $\langle \bar{v} \rangle$  and  $\langle \bar{W} \rangle$  as a function of  $L$  and  $\gamma_0$ . Since the product  $L \langle \bar{v} \rangle$  is much smaller than  $\langle \bar{W} \rangle$  and  $\langle \bar{W} \rangle$  independent of load,  $\eta$  is essentially proportional to  $\frac{L \langle \bar{v} \rangle}{\langle \bar{W} \rangle / \tau}$ . However,  $\langle \bar{W} \rangle$  is a nonmonotonic function

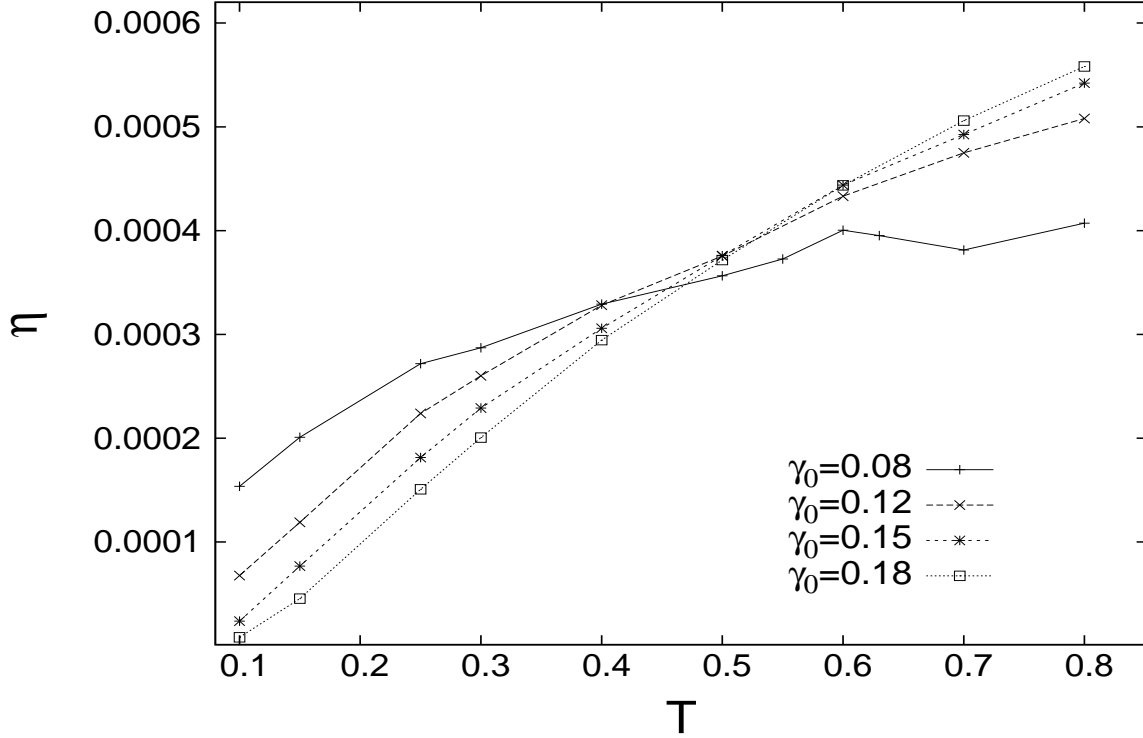


FIG. 17: The figure shows the variation of  $\eta$  as a function of  $T$  for selected values of various  $\gamma_0$  (as indicated in the graph) for constant load  $L = 0.002$  and  $\tau = 8$ . Here  $\lambda = 0.9$ ,  $F_0 = 0.2$  and  $\theta = 0.5\pi$ .

of  $\gamma_0$  and so is  $\langle \bar{v} \rangle$  which, in addition, depends on  $L$ . In the following we present these results in detail separately.

Figure 13 shows  $\langle \bar{v} \rangle$  as a function of  $\gamma_0$  for various values of load  $L$ , at  $T = 0.1$ , for  $\theta = 0.5\pi$  and  $\tau = 8.0$ . It shows that for a given  $L$  below a value  $\gamma_0^{min}$  of  $\gamma_0$  ratchet does not do work against the load and hence the concept of thermodynamic efficiency is not meaningful. In the inset of Fig. 13,  $\gamma_0^{min}$  is plotted as a function of  $L$ .

In Fig. 14 the efficiency  $\eta$  is plotted as a function of  $\gamma_0$  for three values of load  $L = 0.002$ ,  $0.003$  and  $0.005$  and for other parameters same as for Fig. 13. For larger  $L$ , the curves, which peak at intermediate  $\gamma_0$  values, shift to larger  $\gamma_0$  values. From Fig. 14 one can extract two important results. For a given load, for all values of  $\gamma_0$  smaller than the one at which  $\eta$  peaks, ratchets with larger  $\gamma_0$  are more efficient than those with lower damping. In these smaller  $\gamma_0$  regions for a given  $\gamma_0$  efficiency decreases with increasing applied load. However, as  $\gamma_0$  increases  $\eta$  shows nonmonotonic behaviour. The behaviour includes one in which efficiency increases with applied load in the large  $\gamma_0$  region. This counterintuitive

result appears over a vast large- $\gamma_0$  region despite the fact that  $\langle \bar{v} \rangle$  consistently decreases with increasing load,  $L$ , Fig. 13, for any fixed  $\gamma_0$ . This is because, as mentioned earlier,  $\eta$  is essentially proportional to  $L \langle \bar{v} \rangle$ , since  $\langle \bar{W} \rangle$  is independent of  $L$ . And  $L \langle \bar{v} \rangle$  increases as  $L$  increases since the corresponding decrease in  $\langle \bar{v} \rangle$  is smaller in this region of  $\gamma_0$ . This is interesting because more loaded a ratchet is the more efficiently it functions!

As has been pointed out earlier[38],  $\langle \bar{v} \rangle$  increases as a function of noise strength (temperature), becomes maximum at around  $T = 1.0$  and then slowly decreases, when all other parameters are kept fixed. In Fig. 15 we plot  $\langle \bar{v} \rangle$  as a function of  $\gamma_0$  for various temperatures with  $\tau = 8.0$ ,  $\theta = 0.5\pi$  and load  $L = 0.002$ . The curves have the same qualitative features as in case of  $L = 0$ , Fig. 8. It can be seen that, barring at very small  $\gamma_0$  values,  $\langle \bar{v} \rangle$  increases with temperature for any value of  $\gamma_0$  in the range of temperatures ( $T < 1.0$ ) we have explored. The corresponding efficiencies are shown in Fig. 16.

The efficiency  $\eta$  as a function of  $T$  at a fixed  $\gamma_0$  is given in Fig. 17, showing a monotonic increase in the range of  $T$  shown. This shows that larger efficiencies can be obtained at elevated temperatures. However, the increase is likely to stop and even reverse if the temperature is increased further. At low temperatures, smaller  $\gamma_0$  ratchets are more efficient than larger  $\gamma_0$  ratchets. However, at larger temperatures larger  $\gamma_0$  ratchets become more efficient than the smaller  $\gamma_0$  ratchets. Of course, the shown result is for a smaller load of  $L = 0.002$ . However, the qualitative features remain the same for other loads as well.

## V. DISCUSSION AND CONCLUSION

Admittedly, the frictional ratchet discussed here yields very small currents, because it is a kind of minimal model having symmetric periodic potential and driven by a weak subthreshold sinusoidal forcing at a small constant temperature. There are ways, as has been reported earlier[50], to obtain larger ratchet currents using larger amplitude and smaller frequency of sinusoidal driving force at elevated temperatures. However, our purpose has been to study the ratchet currents in the domain of parameter space where the probability of obtaining stochastic resonance also is nonzero. Even in this restricted domain the thermodynamic efficiency of the ratchet against applied load, though small, shows interesting behaviour; efficiency increases with increasing application of load. This is possible only because the input energy extracted from the driving field shows nonmonotonic behaviour and has much larger

magnitude than the product of current and load. Also, intuitively one would feel that as the load is increased the ratchet current should diminish rapidly. This is indeed true in the small friction range. However, as the friction increases the current decreases with increasing load very slowly and thereby sustains current against much larger loads. Moreover, this system also allows us to find how the conventional resonance frequency varies with increasing damping and large amplitude oscillations. This latter aspect will be published elsewhere in detail.

We thank the Computer Centre, North-Eastern Hill University, Shillong, for providing the High Performance Computing Facility, SULEKOR. We are also thankful to the High Performance Computing Laboratory of Computer Science and Engineering Department, National Institute of Technology Meghalaya, for the computing facility PARAMSHAVAK.

- 
- [1] K. Svoboda, C. F. Schmidt, B. J. Schnapp, and S. M. Block, *Direct observation of kinesin stepping by optical trapping interferometry*, 1993 *Nature* **365** 721; J. T. Finer, R. S. Simmons, and J. A. Spudich, *Single myosin molecule mechanics: piconewton forces and nanometre steps*, 1994 *Nature* **368** 113
  - [2] R. P. Feynman, R. Leighton, and M. Sands, 1963 *The Feynman Lectures On Physics*, Vol. 1 Ch. 46, Addison-Wesley Publishing Company Inc.
  - [3] J. Prost, J. F. Chauwin, L. Peliti, and A. Ajdari, *Asymmetric pumping of particles*, 1994 *Phys. Rev. Lett.* **72** 2652
  - [4] M. O. Magnasco, *Forced thermal ratchets*, 1994 *Phys. Rev. Lett.* **71** 1477; 1994 *ibid* **72** 2656
  - [5] P. Reimann, *Brownian motors: noisy transport far from equilibrium*, 2002 *Phys. Rep.* **361** 57
  - [6] P. Hänggi, and F. Marchesoni, *Artificial Brownian motors: Controlling transport on the nanoscale*, 2009 *Rev. Mod. Phys.* **81** 387
  - [7] P. C. Bressloff, and J. M. Newby, *Stochastic models of intracellular transport*, 2013 *Rev. Mod. Phys.* **85** 135
  - [8] P. Jung, J. G. Kissner, and P. Hanggi, *Regular and chaotic transport in asymmetric periodic potentials: Inertia ratchets* 1996 *Phys. Rev. Lett.* **76** 3436
  - [9] J. L. Mateos, *Chaotic transport and current reversal in deterministic ratchets*, 2000 *Phys. Rev. Lett.* **84** 258

- [10] A. Kenfack, S. M. Sweetnam, and A. K. Pattanayak, *Bifurcations and sudden current change in ensembles of classically chaotic ratchets*, 2007 *Phys. Rev. E* **75** 056215
- [11] S. Saikia, and M. C. Mahato, *Deterministic inhomogeneous inertia ratchets*, 2010 *Physica A* **389** 4052
- [12] B. S. Dandogbessi, O. Akin-Ojo, and A. Kenfack, *Controlling current reversals in chaotic ratchet transport*, 2015 *Phys. Scr.* **90** 055206; B. S. Dandogbessi, A. Kenfack, *Absolute negative mobility induced by potential phase modulation*, 2015 *Phys. Rev. E* **92** 062903
- [13] J. Spiechowicz, P. Hanggi, and J. Luczka, *Josephson junction ratchet: The impact of finite capacitances*, 2014 *Phys. Rev. B* **90** 054520; C. M. Falco, *Phasespace of a driven, damped pendulum (Josephson weak link)*, 1976 *Am. J. Phys.* **44** 733; A. Barone, and G. Paterno, *Physics and Applications of the Josephson Effect*, 1982 John Wiley, New York
- [14] J. Spiechowicz, P. Hänggi, and J. Luczka, *Brownian motors in the microscale domain: Enhancement of efficiency by noise*, 2014 *Phys. Rev. E* **90** 032104
- [15] J. Spiechowicz, and J. Luczka, *Efficiency of the SQUID ratchet driven by external current*, 2015 *New J. Phys.* **17** 023054; J. Spiechowicz, and J. Luczka, *Josephson phase diffusion in the superconducting quantum interference device ratchet*, 2015 *Chaos* **25** 053110
- [16] M. Borromeo and F. Marchesoni, *Backward-to-forward jump rates on a tilted periodic substrate*, 2000 *Phys. Rev. Lett.* **84** 203; O. M. Braun and R. Ferrando, *Role of long jumps in surface diffusion*, 2002 *Phys. Rev. E* **65** 061107
- [17] O. M. Braun, A. R. Bishop and J. Roder, *Hysteresis in the underdamped driven Frenkel-Kontorova model*, 1997 *Phys. Rev. Lett.* **79** 3692
- [18] P. K. Ghosh, V. R. Misko, F. Marchesoni, and F. Nori, *Self-propelled Janus particles in a ratchet: Numerical simulations*, 2013 *Phys. Rev. Lett.* **110** 268301; P. K. Ghosh, Y. Li, F. Marchesoni, and F. Nori, *Pseudochemotactic drifts of artificial microswimmers*, 2015 *Phys. Rev. E* **92** 012114
- [19] B. Ai, and F. Li, *Transport of underdamped active particles in ratchet potentials*, 2017 *Soft Matter* **13** 2536
- [20] M. C. Mahato, *Mobility of a forced Brownian particle*, 2004 *Indian J. Phys.* **78** 693
- [21] D. R. Chialvo, and M. M. Millonas, *Asymmetric unbiased fluctuations are sufficient for the operation of a correlation ratchet*, 1995 *Phys. Lett. A* **209** 26; M. C. Mahato, and A. M. Jayanavar, *Synchronized first-passages in a double-well system driven by an asymmetric periodic*

- field, 1995 *Phys. Lett. A* **209** 21
- [22] S. Flach, O. Yevtushenko, Y. Zolotaryuk, *Directed current due to broken time-space symmetry*, 2000 *Phys. Rev. Lett.* **84** 2358; O. Yevtushenko, S. Flach, and K. Richter, *AC-driven phase-dependent directed diffusion*, 2000 *Phys. Rev. E* **61** 7215
- [23] D. Hennig, L. Schimansky-Geier, P. Hänggi, *Slowly rocking symmetric, spatially periodic Hamiltonians: The role of escape and the emergence of giant transient directed transport*, 2008 *Eur. Phys. J. B* **62** 493
- [24] W. L. Reenbohn, and M. C. Mahato, *Net particle current in an adiabatically driven unbiased inhomogeneous inertial system in a periodic potential*, 2009 *J. Stat. Mech.:Theory and Experiment* **03** P03011
- [25] P. J. Martinez, and R. Chacon, *Ratchet universality in the presence of thermal noise*, 2013 *Phys. Rev. E* **87** 062114
- [26] W. L. Reenbohn, and M. C. Mahato, *Dynamical states, stochastic resonance, and ratchet effect in a biharmonically driven sinusoidal potential*, 2015 *Phys. Rev. E* **91** 052151
- [27] M. Büttiker, *Transport as a consequence of state-dependent diffusion*, 1987 *Z. Phys. B - Condensed Matter*, **68** 161
- [28] R. Landauer, *Motion out of noisy states*, 1988 *J. Stat. Phys.* **52** 233
- [29] Ya M. Blanter, and M. Büttiker, *Rectification of fluctuations in an underdamped ratchet*, 1998 *Phys. Rev. Lett.* **81** 4040
- [30] R. Benjamin, and R. Kawai, *Inertial effects in Büttiker-Landauer motor and refrigerator at the overdamped limit*, 2008 *Phys. Rev. E* **77** 051132
- [31] R. Luchsinger, *Transport in nonequilibrium systems with position-dependent mobility*, 2000 *Phys. Rev. E* **62** 1
- [32] G. Wahnstöm, *Diffusion of an adsorbed particle: Theory and numerical results*, 1985 *Surf. Sci.* **159** 311
- [33] D. Dan, A. M. Jayannavar, and M. C. Mahato, *Efficiency and current reversals in spatially inhomogeneous ratchets*, 2000 *International Journal of Modern Physics B*, **14** 1585; D. Dan, A. M. Jayannavar, and M. C. Mahato, *Motion in a rocked ratchet with spatially periodic friction*, 2001 *Physica A* **296** 375; D. Dan, M.C. Mahato, and A.M. Jayannavar, *Multiple current reversals in forced inhomogeneous ratchets*, 2001 *Phys. Rev. E* **63** 056307
- [34] B. Ai, X. Wang, G. Liu, H. Xie, D. Wen, W. Chen, and L. Liu, *Current reversals in an*

- inhomogeneous system with asymmetric unbiased fluctuations*, 2004 *Eur. Phys. J. B* **37** 523
- [35] R. Krishnan, M. C. Mahato, and A. M. Jayannavar, *Brownian rectifiers in the presence of temporally asymmetric unbiased forces*, 2004 *Phys. Rev. E* **70** 021102
- [36] S. von Gehlen, M. Evstigneev, and P. Reimann, *Ratchet effect of a dimer with broken friction symmetry in a symmetric potential*, 2009 *Phys. Rev. E* **79** 031114
- [37] W. L. Reenbohn, S. Saikia, R. Roy, and M. C. Mahato, *Motional dispersions and ratchet effect in inertial systems*, 2008 *Pramana - J. Phys.* **71** 297
- [38] D. Kharkongor, W. L. Reenbohn, and M. C. Mahato, *Particle dynamics in a symmetrically driven underdamped inhomogeneous periodic potential system*, 2016 *Phys Rev. E* **94** 022148
- [39] S. Saikia, *Ratchet effect in an underdamped periodic potential and its characterisation*, 2017 *Physica A* **468** 219
- [40] B. Ai, and L. Liu, *Facilitated movement of inertial Brownian motors driven by a load under an asymmetric potential*, 2007 *Phys. Rev. E* **76** 042103
- [41] J. M. Sancho, M. San Miguel, and D. Duerr, *Adiabatic elimination for systems of Brownian particles with nonconstant damping coefficients*, 1982 *J. Stat. Phys.* **28** 291
- [42] A. M. Jayannavar, and M. C. Mahato, *Macroscopic equation of motion in inhomogeneous media: a microscopic treatment*, 1995 *Pramana - Journal of Physics*, **45** 369
- [43] E. A. Desloge, *Relation between equations in the international, electrostatic, electromagnetic, Gaussian, and Heaviside Lorentz systems*, 1994 *Am. J. Phys.* **62** 601
- [44] W. H. Press, B. P. Flannery, S. A. Teukolsky, and W. T. Vetterling, Numerical Recipes, 1987 Cambridge University Press, Cambridge, England
- [45] M. C. Mahato, and S. R. Shenoy, *Hysteresis loss and stochastic resonance: A numerical study of a double-well potential*, 1994 *Phys. Rev. E* **50** 2503; T. Iwai, *Study of stochastic resonance by method of stochastic energetics*, 2001 *Physica A* **300** 350; M. Evstigneev, P. Reimann, C. Schmitt, and C. Bechinger, *Quantifying stochastic resonance: theory versus experiment*, 2005 *J. Phys.: Condens. Matter* **17** S3795
- [46] R. Mannella, *A Gentle Introduction to the Integration of Stochastic Differential Equations*, Edited by J. A. Freund and T. Pöschel, 2000 Lecture Notes in Physics, Vol. **557**, 353. Springer, Berlin
- [47] K. Sekimoto, *Kinetic characterization of heat bath and the energetics of thermal ratchet models*, 1997 *J. Phys. Soc. Jpn.* **66** 1234

- [48] S. Saikia, A. M. Jayannavar, and M. C. Mahato, *Stochastic resonance in periodic potentials*, 2011 *Phys. Rev. E* **83** 061121
- [49] W. L. Reenbohn, S. S. Pohlong, and M. C. Mahato, *Periodically driven underdamped periodic and washboard potential systems: Dynamical states and stochastic resonance*, 2012 *Phys. Rev. E* **85** 031144
- [50] Large values of  $\langle \bar{v} \rangle$  have been obtained for large  $\tau$  values when driven by large amplitude field  $F(t)$  at elevated temperatures. See Ph.D. thesis (2010) of S. Saikia submitted to North-Eastern Hill University, Shillong, India.